

Design and Testing of an Active Core for Sandwich Panels

Jiangzi Lin, Liyong Tong and Zhen Luo

School of Aerospace, Mechanical and Mechatronic Engineering
The University of Sydney
NSW 2006 Australia

March 2008

Report Documentation Page				Form Approved OMB No. 0704-0188	
Public reporting burden for the collection of information is estimated to average 1 hour per response, including the time for reviewing instructions, searching existing data sources, gathering and maintaining the data needed, and completing and reviewing the collection of information. Send comments regarding this burden estimate or any other aspect of this collection of information, including suggestions for reducing this burden, to Washington Headquarters Services, Directorate for Information Operations and Reports, 1215 Jefferson Davis Highway, Suite 1204, Arlington VA 22202-4302. Respondents should be aware that notwithstanding any other provision of law, no person shall be subject to a penalty for failing to comply with a collection of information if it does not display a currently valid OMB control number.					
1. REPORT DATE 22 AUG 2008		2. REPORT TYPE Final		3. DATES COVERED 31-10-2006 to 30-10-2007	
4. TITLE AND SUBTITLE Active Pin Reinforced Sandwich Panels				5a. CONTRACT NUMBER FA48690710009	
				5b. GRANT NUMBER	
				5c. PROGRAM ELEMENT NUMBER	
6. AUTHOR(S) Liyong Tong				5d. PROJECT NUMBER	
				5e. TASK NUMBER	
				5f. WORK UNIT NUMBER	
7. PERFORMING ORGANIZATION NAME(S) AND ADDRESS(ES) University of Sydney, Department of Aeronautical Engineering, Sydney , Australia, NA, NSW 2006				8. PERFORMING ORGANIZATION REPORT NUMBER N/A	
9. SPONSORING/MONITORING AGENCY NAME(S) AND ADDRESS(ES) AOARD, UNIT 45002, APO, AP, 96337-5002				10. SPONSOR/MONITOR'S ACRONYM(S) AOARD	
				11. SPONSOR/MONITOR'S REPORT NUMBER(S) AOARD-064085	
12. DISTRIBUTION/AVAILABILITY STATEMENT Approved for public release; distribution unlimited					
13. SUPPLEMENTARY NOTES					
14. ABSTRACT This report presents a study on analysis, design and testing of an active core of a sandwich panel for achieving maximum bending morphing. Firstly, a SIMP-PP algorithm is developed by combining the SIMP method and the physical programming for topology design of complaint mechanisms and then validated via a number of selected numerical examples. Secondly, a unit cell concept is established for the overall shape morphing of single unit cell for the purpose of conducting topology optimization of an active core, and then multiple unit cells connected in a series manner to form the core are assessed numerically to understand its capability of shape morphing. Thirdly, a prototype of three unit cell core was fabricated using rapid prototyping for experimental demonstrating the morphing capability. Preliminary testing results show that the cantilever core can achieve a maximum tip deflection angle of approximately 10 degrees.					
15. SUBJECT TERMS					
16. SECURITY CLASSIFICATION OF:			17. LIMITATION OF ABSTRACT Same as Report (SAR)	18. NUMBER OF PAGES 50	19a. NAME OF RESPONSIBLE PERSON
a. REPORT unclassified	b. ABSTRACT unclassified	c. THIS PAGE unclassified			

REPORT DOCUMENTATION PAGE				Form Approved OMB No. 0704-0188	
Public reporting burden for this collection of information is estimated to average 1 hour per response, including the time for reviewing instructions, searching existing data sources, gathering and maintaining the data needed, and completing and reviewing this collection of information. Send comments regarding this burden estimate or any other aspect of this collection of information, including suggestions for reducing this burden to Department of Defense, Washington Headquarters Services, Directorate for Information Operations and Reports (0704-0188), 1215 Jefferson Davis Highway, Suite 1204, Arlington, VA 22202-4302. Respondents should be aware that notwithstanding any other provision of law, no person shall be subject to any penalty for failing to comply with a collection of information if it does not display a currently valid OMB control number. PLEASE DO NOT RETURN YOUR FORM TO THE ABOVE ADDRESS.					
1. REPORT DATE (DD-MM-YYYY) 28 March 2008		2. REPORT TYPE Final		3. DATES COVERED (From - To) 31 Oct 06 - 31 Oct 07	
4. TITLE AND SUBTITLE Design and Testing of an Active Core for Sandwich Panels				5a. CONTRACT NUMBER FA4869-07-1-0009	
				5b. GRANT NUMBER	
				5c. PROGRAM ELEMENT NUMBER	
6. AUTHOR(S) Jiangzi Lin, Liyong Tong and Zhen Luo				5d. PROJECT NUMBER	
				5e. TASK NUMBER	
				5f. WORK UNIT NUMBER	
7. PERFORMING ORGANIZATION NAME(S) AND ADDRESS(ES) School of Aerospace, Mechanical & Mechatronics Eng., University of Sydney, NSW 2006 Australia				8. PERFORMING ORGANIZATION REPORT NUMBER FEARC-08-001	
9. SPONSORING / MONITORING AGENCY NAME(S) AND ADDRESS(ES) Air Force Research Laboratory AFOSR/AOARD 7-23-17 Roppongi Minato-ku, Tokyo 106-0032 Japan				10. SPONSOR/MONITOR'S ACRONYM(S)	
				11. SPONSOR/MONITOR'S REPORT NUMBER(S)	
12. DISTRIBUTION / AVAILABILITY STATEMENT					
13. SUPPLEMENTARY NOTES					
14. ABSTRACT This report presents a study on analysis, design and testing of an active core of a sandwich panel for achieving maximum bending morphing. Firstly, a SIMP-PP algorithm is developed by combining the SIMP method and the physical programming for topology design of complaint mechanisms and then validated via a number of selected numerical examples. Secondly, a unit cell concept is established for the overall shape morphing of single unit cell for the purpose of conducting topology optimization of an active core, and then multiple unit cells connected in a series manner to form the core are assessed numerically to understand its capability of shape morphing. Thirdly, a prototype of three unit cell core was fabricated using rapid prototyping for experimental demonstrating the morphing capability. Preliminary testing results show that the cantilever core can achieve a maximum tip deflection angle of approximately 10 degrees.					
15. SUBJECT TERMS Sandwich panels, Active core, topology optimization,					
16. SECURITY CLASSIFICATION OF:			17. LIMITATION OF ABSTRACT SAR	18. NUMBER OF PAGES	19a. NAME OF RESPONSIBLE PERSON
a. REPORT unclassified	b. ABSTRACT unclassified	c. THIS PAGE unclassified			19b. TELEPHONE NUMBER (include area code)

Summary

This report presents a study on analysis, design and testing of an active core of a sandwich panel for achieving maximum bending morphing. Firstly, a SIMP-PP algorithm is developed by combining the SIMP method and the physical programming for topology design of compliant mechanisms and then validated via a number of selected numerical examples. Secondly, a unit cell concept is established for the overall shape morphing of single unit cell for the purpose of conducting topology optimization of an active core, and then multiple unit cells connected in a series manner to form the core are assessed numerically to understand its capability of shape morphing. Thirdly, a prototype of three unit cell core was fabricated using rapid prototyping for experimental demonstrating the morphing capability. Preliminary testing results show that the cantilever core can achieve a maximum tip deflection angle of approximately 10 degrees.

Table of content

TABLE OF CONTENT	4
1 INTRODUCTION	5
2 FUNDAMENTALS FOR DESIGNING ENGINEERED ACTIVE CORE.....	8
2.1 CONCEPTUAL DESIGN OF UNIT CELL STRUCTURE	8
2.2 MODEL OF A UNIT CELL AND ITS MECHANICS.....	9
2.2.1 <i>Topology optimization</i>	9
2.2.2 <i>Compliant mechanism</i>	10
2.3 A NEW MULTI-OBJECTIVE OPTIMIZATION SCHEME SIMP-PP	12
2.3.1 <i>Physical programming</i>	13
2.3.2 <i>Flowchart for SIMP-PP</i>	17
2.3.3 <i>Formulation of SIMP-PP for compliant mechanism</i>	19
2.4 NUMERICAL EXAMPLES OF USING SIMP-PP IN STRUCTURAL DESIGN	22
2.4.1 <i>Compliant inverter</i>	23
2.4.2 <i>Compliant gripper</i>	28
3 DESIGN OF SANDWICH CORE ARCHITECTURE FOR SHAPE MORPHING	33
3.1 MODELING AND DESIGN OF SINGLE UNIT CELL.....	33
3.1.1 <i>Design criteria</i>	33
3.1.2 <i>Loading conditions</i>	34
3.1.3 <i>Boundary conditions and connectivity conditions</i>	35
3.1.4 <i>Material interpolation</i>	35
3.1.5 <i>Objective function and sensitivity analysis</i>	36
3.1.6 <i>Remarks</i>	37
3.1.7 <i>An illustrative example</i>	38
3.2 ASSEMBLING OF MULTIPLE UNIT CELLS	40
4 DEMONSTRATIVE TESTING	42
4.1 POST PROCESSING AND PROTOTYPING.....	42
4.2 EXPERIMENT	44
4.2.1 <i>Test set-up</i>	44
4.2.2 <i>Results and discussion</i>	45
5 CONCLUSIONS.....	48
REFERENCE	49

1 Introduction

Driven by the demand and the need for aircraft to achieve greater efficiency in terms of maneuverability, adaptability, and cost savings. The research on design, analysis and development of adaptive morphing aircraft structures becomes a focus in the aerospace research sector. The adaptive airfoil or morphing wing or smart wing is generally perceived as the source to achieve greater level of efficiency because of its significant impact on aircraft performance and aircraft operations. The airfoils on an aircraft generally account for more than 95% of the total lift and 40% of the drag, however, current airfoils are designed as relatively static structures that do not possess the ability to alter its effectiveness to the ever changing flight conditions; the core of the adaptive airfoil concept is to have the ability to alter the geometry of an airfoil and thus directly affect its effectiveness during various flight environments. An adaptive airfoil requires an optimally designed internal structural architecture sandwiched between upper and lower wing skins that can changes its geometry in response to flight operation requirements. Hence, this research project aims to develop fundamental concepts and understanding on design and analysis of active core in a sandwich panel which hopefully can offer a perspective on the design of adaptive airfoils with the use of topology optimization; it presents an exploratory design approach for compliant airfoil structures based on topology optimization of compliant unit cell structures. This approach focuses the optimization on a comparatively small compliant unit cell that has the ability to actuate local deflection; by combining networks of linked unit cells the sandwich core structure can be synthesized and large camber deflections can be achieved through the accumulation of local deflections in the network.

Design of smart internal structures for airfoils has attracted an attention of many researchers. Most of the airfoil structure designs adopt compliant mechanism concept and are achieved intuitively based on experience, intuition and trial and error. (Munday and Jacob 2001) designed and tested a compliant airfoil with embedded PZT layer in the pursuit of flow control via variable camber. (Stanewsky 2001) considered various compliant airfoil designs, using both conventional and smart material actuators to achieve flow control for various types of airfoils. (Cho, Wong et al. 2004) constructed an ultrasonic motor driven trailing edge control surface for camber and twist control. (Campanile and Anders 2005) designed and prototyped a so called “belt-rib” airfoil for compliant camber control with unique

internal architecture that exploit the structural flexibility of the airfoil while simultaneously maintaining its load carrying features. (Ramrakhyani, Lesieutre et al. 2005) designed and modeled a high authority compliant wing with internal structure composed of cellular trusses. (Raja and Upadhyaya 2007) designed and tested a compliant airfoil with stack PZT actuators in the active control of wing flutter suppression.

Structural topology optimization has also been used in the internal structure design of adaptive airfoil. The potential advantage of applying topology optimization in compliant airfoil structures is that the design problem can be formulated using mathematical formulations that are physically meaningful, and the final topology can be achieved through an iterative and systematic material distribution method that relies on the sensitivity analysis of the objective function with respect to the design variables. Thus the degree of intuition based or experience based decision making is decreased, which is arguably an advantage when designing novel structures such as compliant airfoils, since limited experience can be extracted from previous work.

Thus this research project is an exploratory study in the feasibility of using topology optimization in the design of compliant airfoil structures for the specific function of achieving camber deflection. It consists of two parts, theoretical concepts and formulations, and experimental demonstration.

In the theoretic aspect, PZT driven actuation is considered by defining PZT material as the active material in the bi-material design. PZT driven compliant mechanism designs become popular in the field of topology optimization due to that PZT materials are commercially available and can be attached to the host structure rather easily through adhesive bonds. However, the actuation energy and the actuation strain of PZT material are generally less than that of the shape memory alloy (SMA). Another focus in this part is the expansion in the topology optimization of compliant mechanism; thus far the biomaterial designs have offered solutions with varying degree of unimorph mechanism and tension/compression mechanism. As of yet the designer typically have no control over the extent of employment of the two mechanism through explicit means. The current research focus is aimed at formulating a strategy to ensure a pure tension/compression driven compliant mechanism so as to eliminate the presence of uni-morph mechanisms. It is noted that the resulting topology

often gives a complex geometry with high degrees of unimorph; however due to the current fabrication technologies and the forms of commercially available actuation systems the practicality of these designs have come into scrutiny, and often post-processing needs to be carried out to remove some degrees of unimorph from the design.

In the experiment, the current prototype, which is made of polycarbonate material and Nitinol spring actuators, has been successfully tested and is able to achieve tip deflection angles of approximately 10 degrees.

2 Fundamentals for designing engineered active core

2.1 *Conceptual design of unit cell structure*

This project focuses on the conceptual design on a cellular level, which would form the building block of the sandwich core or the internal wing structure. The principal of the cellular design is to achieve the desired global shape change through the local deformation of multiple unit cells.

A unit cell structure is a building block used in the assembly of a larger, global structure through repeatedly linked networks. It is required to carry the generic performance feature of the global structure (such as camber deflection), and by skilled design this feature can be accumulated and magnified over a network of repeatedly linked cells. Certain unit cell structures such as the Kagome truss (Hutchinson, Wicks et al. 2003; Symons, Hutchinson et al. 2005) holds potential in the design of morphing structures that require the structure to be stiff under external loading while possess the ability to carry out large deformation under internal actuation (selective deformation of local components within the unit cell).

Compliant unit cell networks have the advantage of distributing the compliance across a large region of the airfoil, thus avoiding stress concentration in a single pivoting point as well as avoiding flow separation due to a sudden change in geometry and achieve finer deflection authority over large portions of the airfoil. A single cell may not achieve significant amount of deformation on its own, but through its connections with the adjacent cells the deformation can be “passed on” to the next cell, and the combined deformation of the two cells can be passed on to the third cell, and so large global deformation can be achieved over networks of unit cell structures through the accumulation of local deformation of each unit cell. This is a very important feature for an adaptive sandwich core or an airfoil, the change in camber should be achieved steadily over a substantial portion of the chord rather than a sudden change at a pivoting point; a sudden change in deflection angle could induce flow separation whereas a gradual deflection helps remains laminar flow.

In this study the unit cell design is conducted on a bi-material smart structure setup. The bi-material setup is so that there is one passive material which makes up the majority of the structure, and one smart material that is placed at specific locations in the unit cell network

to serve as the actuation material. The shape memory alloy, such as Nitinol, is chosen due to its greater shape memory strain (8.5%), practical fabrication technique, and is relatively inexpensive.

2.2 Model of a unit cell and its mechanics

The design of the compliant adaptive core structure is conducted through topology optimization. The concepts involving topology optimization and its application to compliant structures are reviewed and discussed in the following sections.

2.2.1 Topology optimization

Topology optimization refers to the advance structural optimization methods that are capable of determining both the size and shape of the structure, given specified functionalities and constraints. The field of topology optimization has experienced steady advancement in the last decade with many different schemes such as the material distribution approach (Bendsoe and Kikuchi 1988; Bendsoe and Sigmund 1999), the implicit free boundary representation method (Wang, Wang et al. 2003; Allaire, Jouve et al. 2004), the evolutionary structural optimization (ESO) method (Xie and Steven 1993), and genetic algorithm (GA) method (Tang, Tong et al. 2005) and so on. Amongst those methods, the SIMP method (Bendsoe and Kikuchi 1988; Bendsoe and Sigmund 1999) is adopted here.

SIMP has been widely accepted and had various successful applications across a board spectrum of disciplines including aerospace design (Maute and Allen 2004). It features implementation ease and computation efficiency, and has readily available convergence algorithms. The core of the SIMP scheme evolves around converting the original classic structural optimization problem with discrete design variables (variables either be 0 or 1) to a continuum optimization scheme with continuous design variables (variables occupy the range from 0 to 1). In doing so, many well-founded gradient based convergence algorithms, such as the Optimal Criteria (OC) method (Zhou and Rozvany 1991) and the Method of Moving Asymptote (MMA) (Svanberg 2002), can be applied to the large scale optimization problem. Mathematically, SIMP uses a nonlinear relationship to relate the material properties to the element densities as

$$E(x) = E_{\min} + x_j^p (E_0 - E_{\min}) \quad (1)$$

where E_0 and E_{\min} represent material properties of solid and void components, respectively. The design variable x_j ($0 < x_j \leq 1$) acts as the relative density to the intrinsic material density by allowing intermediate values between its prescribed binary bound. The penalty factor p is used to recover the original binary material distribution by satisfying some simple conditions (Bendsoe and Sigmund 1999) to enforce intermediate element densities towards its prescribed bounds. In numerical implementation of this study, $p = 3$ is used. The mathematical programming tool adjusts each design variable iteratively and at the end of the optimization procedure all the design variables will obtain binary status with either 1, representing solid material; or close to 0 to represent void (To avoid numerical singularity, 0.0001 is applied as the minimization rather than 0).

2.2.2 Compliant mechanism

The possible applications of topology optimization are numerous, but the synthesis of compliant mechanisms (Howell 2001) is one of such attractive areas to which the topology optimization technology has been popularly applied in the last few years (Ananthasuresh, Kota et al. 1994; Sigmund 1997; Kota, Lu et al. 2005). A compliant mechanism is defined generally as a single piece mechanical device that accomplishes its functions - transferring of motion, force or energy via the flexibility of its component members. It is the strain energy stored in the structure that enables the compliant mechanism to conduct its motion analogous to its mechanical counterpart. However, what makes the compliant mechanisms different from the standard rigid-link mechanisms is that the stored strain energy acts as a built-in restoring force that restores the compliant mechanism to its pre-deformed layout once the applied load is removed, giving it a distinct appeal especially in many areas with actuators. The design of compliant mechanisms is interesting partially because of its inherent multi-objective performance demand (Rahmatalla and Swan 2005; Luo, Yang et al. 2006; Tai and Prasad 2007); on one hand the compliant mechanism needs to suffice its mechanical functionalities with flexibility or displacement output, while on the other hand stiff enough to sustain external loads or force output. The design approach for synthesizing compliant mechanisms can be classified generally into two different types (Howell 2001). One of which is the design of lumped compliant mechanisms based on kinematics analysis approach where the pseudo-rigid-body model is utilized to aid the design of compliant structures in

composed rigid-link components and flexible pivots. The other method is a continuum based approach for the design of so-called distributed compliant mechanisms (Yin and Ananthasuresh 2003) initially rooting from continuum topology optimization of the homogenization approach (Ananthasuresh, Kota et al. 1994), where the designer focuses on determining the topology, shape and size of the unknown structure with distributed compliance.

Significant research efforts on compliant mechanisms are concerned with defining an appropriate objective function so as to express the desired multi-objective performance characteristics. This is of special focus in this project due to the multi-disciplinary nature of aerospace engineering. A compendium of previous work on multi-objective optimization of compliant mechanisms using topology optimization is given below.

As to date, there are two predominate types in problem formulation in the topology optimization of compliant mechanisms, one of which is based on a structural perspective in which the combination of mutual strain energy (MSE, also known as the mutual potential energy MPE), the strain energy (SE) or the equivalent performance measures are used as the objective function vector to quantify mechanical flexibility and structural stiffness respectively, and the final optimization is conducted with respect to a single objective function formed by functional transformation via either weighted sum, ratio, powered ratio, or compromising programming approach (Frecker, Ananthasuresh et al. 1997; Nishiwake, Frecker et al. 1998; Saxena and Ananthasuresh 2000). Alternatively, based on the concept of the kinematics synthesis of conventional rigid-body mechanisms (Sigmund 1997), typical measures such as mechanical advantage (MA, the ratio of input and output force) (Canfield and Frecker 2000) or geometric advantage (GA, the ratio of input and output displacement) (Lau, Du et al. 2001) are used as objective functions to control mechanical force and displacement outputs, so as to implicitly control the structural stiffness and the flexibility individually. As a result, mechanical efficiency (ME, the product of MA and GA) is used as a comprehensive objective function to obtain a balanced trade-off between stiffness and flexibility (Luo, Tong et al. 2007).

In general it is rare that all the individual objectives in a multi-objective optimization routine can be optimized simultaneously thus a unique optimal solution cannot be achieved. It is

therefore a matter of making trade-off decisions to obtain a set of compromising solutions. The concept of Pareto solution is commonly used in addressing the set of compromising solutions of multi-objective optimization problems (Marler and Arora 2004). The definition for Pareto set states that the design point will be chosen as optimal if no criterion can be improved without detriment to at least one other criterion. The weighted sum method (Ananthasuresh, Kota et al. 1994; Nishiwake, Frecker et al. 1998) is known as the simplest and easiest one amongst a variety of multi-objective optimization formulations, which is numerically implemented by minimizing a linear combination of all criteria subject to non-negative weighting factors. To avoid generating an ill-conditioned problem when objective functions are nonlinearly dependent on the design variables, the weighting coefficients must be adequately adjusted during the optimization process to find the set of Pareto optimum solutions. However, this method cannot ensure finding all Pareto solutions for non-convex optimization problems (Chen, Sahai et al. 2000). The reason is that it is difficult to capture the whole Pareto characteristics when Pareto points are linearly distributed, and a uniform variation of the weighting factors often leads to an uneven distribution of the Pareto optimum solutions. Compromising programming scheme and fuzzy-goal programming were also applied as alternative multi-objective methods for topology optimization problems in which the desired set of Pareto solutions can be obtained by varying the corresponding weighting factors for both convex and non-convex optimization problems. Furthermore (Tai and Prasad 2007) proposed a multi-objective topology optimization method for compliant mechanisms using genetic algorithms. (Marler and Arora 2004) gave a comprehensive survey for different multi-objective optimization schemes.

2.3 *A new multi-objective optimization scheme SIMP-PP*

From early review it is concluded that the weighted sum method and the functional transformation methods are generally in-adequate for our problems due to the restriction on that the objectives must share similar physical qualities for the transformation to be meaningful. Thus through this research project a new multi-objective optimization scheme is proposed, which is named as SIMP-PP. It can be regarded as being a partnership between the continuous topology optimization method SIMP and the multi-objective optimization scheme PP (Messac 1996), although it must be noted that the PP scheme is vastly adaptable and can be incorporated into other topology optimization schemes such as the

homogenization and level set methods in general. SIMP interpolation scheme is a widely adopted scheme with a wide range of successful applications (Rozvany 2001), while PP is an alternative multi-objective formulation scheme based on nonlinear programming to transfer multiple objectives into a new single aggregate objective. As far as nonlinear multi-objective optimization is concerned, the primary goal is to appropriately describe the decision maker's preference which is used to model the relative importance of objectives. Amongst various available multi-objective transforming schemes, PP is the one of the effective methods capable of directly expressing a lucid deterministic preference by specifying ranges of desirability based on the availability of design information (Messac and Wilson 1998; Messac, Dessel et al. 2004), and it places special emphasis on the uncertainty nature of design and the robustness of problem formulation in the face of multi-objective, multi-disciplinary problems with the introduction of a relaxed, non-dimensional, generic class function framework. PP has been proven to be effective to suit "real world" complex optimization problems, and it also enjoys the theoretical advantage in its ability in capturing the entire Pareto set for both convex and non-convex problems. However, PP has yet to be utilized in multi-objective topology optimization of compliant mechanisms until now from available publications.

2.3.1 Physical programming

In physical programming, the designer assigns sets of ranges that each objective function is desired to take as well as based on its design requirement to reflect its preference. Each objective $f_i(x)$ is mapped to a strictly positive, non-dimensional scale representing its priority by a class function $\overline{f}_i(f_i(x))$, which is piece-wise to reflect the desirability of the objective according to the range it lies. There are eight possible class functions arranged into four pairs based on different optimization operations on the objective, which are listed as follows:

- Class 1: Minimize
- Class 2: Maximize
- Class 3: Equate to
- Class 4: Lie within range

Each pair has a soft class and a hard class as depicted in

Table 1, with the hard classes representing un-compromising design scenarios with only two discrete preferences (feasible and infeasible) that are intended to function as constraints. The soft classes represent a more flexible design scenario with continuous class functions to reflect varying degrees of desirability. For each class in the problem, the set of ranges is defined by the designer as prior articulation of preferences. The most common class 1-S has a set of six ranges defined in Table 2 and displayed in Figure 1. Class 2-S also has six ranges, Class 3-S and 4-S have 10 and 11 ranges respectively. In PP the more desirable solution will map to a smaller class function value, as shown in Figure 1, with the utopia point being \bar{f} equals to zero.

Table 1 Classification of class functions

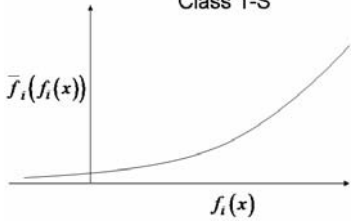
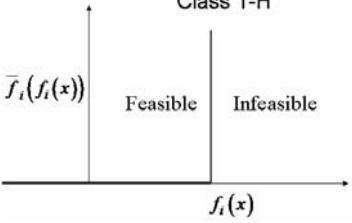
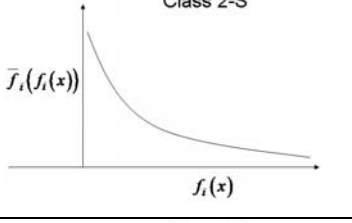
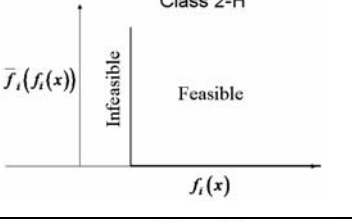
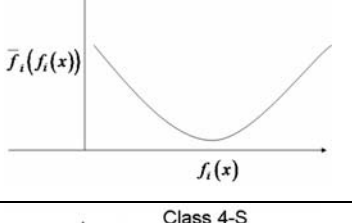
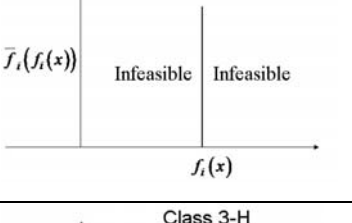
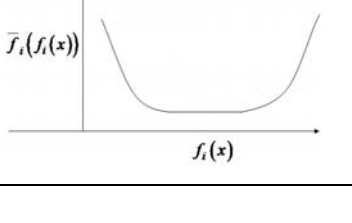
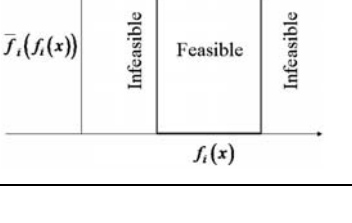
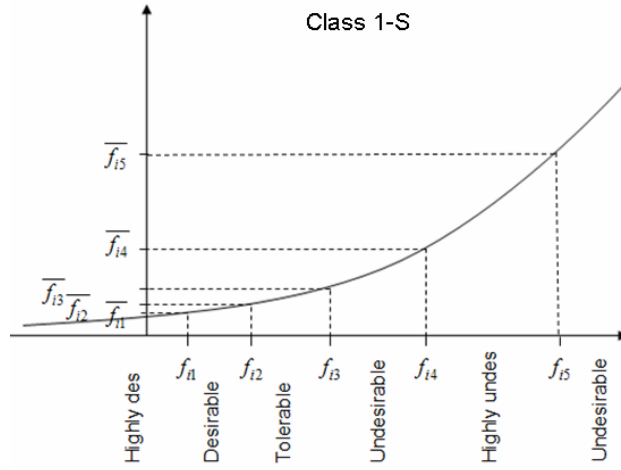
	Soft	Hard
Class 1: Minimize	<p>Class 1-S</p> 	<p>Class 1-H</p> 
Class 2: Maximize	<p>Class 2-S</p> 	<p>Class 2-H</p> 
Class 3: Equate to	<p>Class 3-S</p> 	<p>Class 3-H</p> 
Class 4: Lie within range	<p>Class 4-S</p> 	<p>Class 3-H</p> 

Table 2 Set of preferences for class 1-S

Definition	Range
Highly Desirable	$f_i(x) \leq f_{i1}$
Desirable	$f_{i1} \leq f_i(x) \leq f_{i2}$
Tolerable	$f_{i2} \leq f_i(x) \leq f_{i3}$
Undesirable	$f_{i3} \leq f_i(x) \leq f_{i4}$
Highly Undesirable	$f_{i4} \leq f_i(x) \leq f_{i5}$
Unacceptable	$f_i(x) > f_{i5}$

Figure 1 Class function ranges for the i -th objective

Under PP, the final overall design value is represented by a single multi-attribute function, given by the transformation as follows:

$$f_a(x) = \log \left(\frac{1}{n} \sum_{i=1}^n \bar{f}_i(f_i(x)) \right) \quad (2)$$

With n representing the number of objective functions under optimization and f_a is the aggregate class function.

In theory, PP holds several advantages over other multi-objective optimization schemes:

Firstly, on the issue of Pareto optimality, Messac (Messac 1996) demonstrated this method's sufficiency for Pareto optimality and the ability to capture the complete Pareto frontier with even distribution of points. Chen et al (Chen, Sahai et al. 2000) further conducted a comprehensive study on the Pareto optimality features of PP with comparisons with the weighted sum method and compromise programming method, through the illustration of Pareto frontiers it was shown that PP may be one of the most effective methods in capturing Pareto points under both convex frontier and non-convex frontier. PP shares certain philosophical connections with goal programming and compromise programming in articulating preferences; Compromise programming was used in topology optimization for its capability in capturing the entire Pareto frontier, however compromise programming requires the prior knowledge of utopia points in the objective criterion space such that all objectives are at their best possible solution, which is often unavailable or computationally costly. Therefore, the utopia points are often replaced by aspiration points based on approximation or prediction, and Pareto optimality holds so long as the aspiration point z is out side the feasible criterion space Z , however it can be computationally costly to determine $z \notin Z$ for each objective. Goal programming methods in general suffers the same drawback as compromise programming in topology optimization problems, in that the goal must be un-attainable in order to satisfy Pareto optimality. However, unlike goal programming and compromise programming methods, the articulation of preferences in PP does not need to satisfy $z \notin Z$ and can still achieve Pareto optimality.

Secondly, the class function transformations allow PP to be able to effectively optimize objective functions with different qualitative properties at several orders of magnitude apart. This is an advantage to the functional transformation method. Even though the set of $f_i(x)$ in each class function can be highly non-linear and at different magnitudes, the numerical effect on the class function values when different objectives reach the same degree of desirability in their respective preference range are identical, thus provides a meaningful basis for comparing the desirability of multiple objectives. The same advantage holds for the derivatives of the objective function as well through the transformation of the derivative via the chain rule in Equation (3).

$$\frac{\partial \bar{f}_i(f_i(x))}{\partial x} = \frac{\partial \bar{f}_i(f_i(x))}{\partial f_i} \frac{\partial f_i}{\partial x} \quad (3)$$

In addition Messac (Messac 1996) presented a set of numerical procedures in formulating monotonously increasing/decreasing soft class functions with high nonlinearity, thus allowing the designer to capture the differing degrees of nonlinearity in the desirability of individual objectives. Furthermore, its aggregate function formulation in Equation (2) implicitly emphasize the optimization of the objective with the least desirable preference, which insures benefits of optimizing the overall performance, while at the same time minimize the variance in the desirability of the individual performance.

Thirdly, the articulation of preferences in PP is physically meaningful, where a designer can express the preferences in identical units as the objective function, allowing the designer to make effective use of all available performance requirements. In addition the expression of the preferences in sets of ranges allows for deliberate imprecision in the problem statement, avoiding not sufficing Pareto optimality and offering a flexible comparison for the relative performance of objectives. However as pointed out in (Marler and Arora 2004), when the design information is insufficient then it would require an experienced designer to assign the preferences with accuracy (arguably in ad-hoc fashion). In this case the performance of SIMP-PP would possibly be hindered and in the likely event, reassignment of preferences would be required in similar fashion to weight tweaking. Regardless, it would be presumptuous to expect any multi-objective methods to have outstanding performance under all scenarios, and here we propose SIMP-PP as an alternative and a potential multi-objective scheme for structural topology optimization problems.

2.3.2 Flowchart for SIMP-PP

This following section will combine the typical SIMP and PP schemes into the SIMP-PP multi-objective transformation scheme. For the sake of numerical simplicity linear elastic structure analysis is presented but without losing the generality, even though nonlinear responses are important in practical designs of large-displacement compliant mechanisms. The geometric non-linearity analysis have been achieved and was successfully applied to single material, single objective optimization of compliant mechanisms, it is purely a matter of computation cost concern that prevents its application in more complex topology optimization cases.

The algorithm flowchart for the implementation of SIMP-PP is given in Figure 2 and is explained in the following discussion. In SIMP-PP, the implementation of PP causes additional minor computational efforts in various stages of the optimization process. The range of preferences for each objective are declared before the initiation of the loop, and the class function parameters such as its slope (first derivative), range, and constants are evaluated. It is the compatibility reason that the hard classes in the system to be treated as constraints, and be evaluated in the same fashion as those in typical SIMP analysis, this is due to the fact that in typical SIMP formulation the satisfaction of constraints are generally guaranteed, and also because of numerically motivated reasons when employing MMA as the gradient search algorithm. Initially within the loop, the finite element analysis and the evaluation of objective functions are carried out as in typical SIMP fashion. Once all objective functions f_i are solved the class function is applied to map each objective function to a strictly positive, non-dimensional scale that represents its degree of desirability as shown in Figure 1. For more details of the procedures, the readers are referred to Messac (Messac 1996).

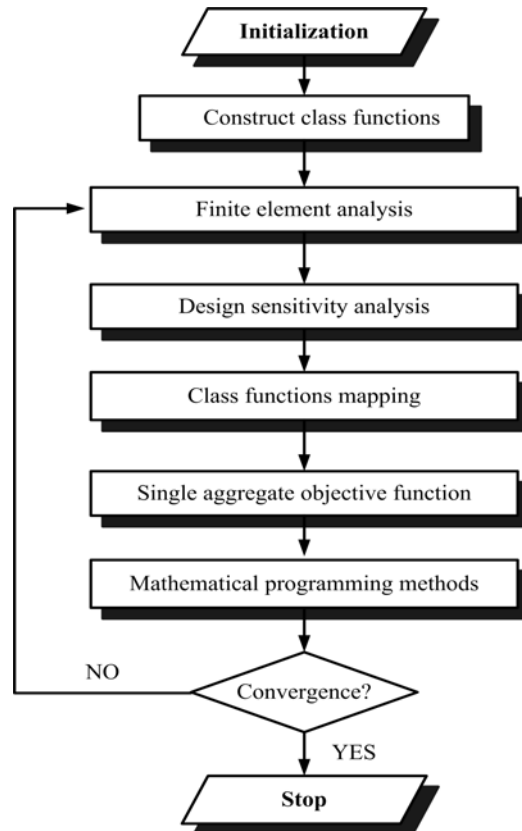


Figure 2 Flowchart for SIMP-PP algorithm

The mappings of the objective functions to the class functions and also its derivatives are of crucial importance in physical programming. The development of the class function is non-unique, so long as the class function adheres to certain properties outlined by Messac (Messac 1996). Thus far in this project, the class functions are of piecewise nature with exponentials and 4th order splines, and shown in Equation (7). Follow on the aggregate objective is calculated according to Equation (2).

In topology optimization of compliant mechanisms, the artificial spring model (Sigmund 1997) attached at the output port is used to model the reaction force from a work-piece. The input actuation is simulated with the applied load f_{in} . In doing so, the desired motion can be obtained at the output port. However, if only the mechanical flexibility is considered in the optimization formulation a very weak and fragile compliant structure will be produced. Therefore, the structural function of minimizing the mean compliance or strain energy (SE) is included to guarantee the compliant mechanism is sufficient to resist reaction force and to maintain its shape when contacting the work-piece. Thus, a more reasonable way for the design of compliant mechanisms is to consider both mechanical flexibility and structural stiffness when formulating the optimization problem.

2.3.3 Formulation of SIMP-PP for compliant mechanism

We formulate the SIMP-PP optimization of compliant mechanisms based on the widely adopted MSE-SE criteria. However in most compliant mechanism design, the objective formulation is based on modifying the MSE-SE coupling by replacing MSE with displacement output u_{out} to characterize flexibility, but as indicated by Bruns and Tortorelli (Bruns and Tortorelli 2001), MSE and u_{out} actually serve as the same objective function for linear elastic structures, while for geometrically nonlinear structures it is not obvious that these two objective measurements are the same. The popularly studied MSE-SE formulation characterizes the flexibility-stiffness performance of the compliant structure through functional transformation and optimality condition is based on the premise that the continuum stiffness is linear in the design variables. However, it is important to note that although the formulation in this work is based on linear model, it in no means restricts the application of the proposed SIMP-PP from nonlinear models because any set of objective functions f_i rather than just MSE-SE can be transformed into one aggregate function using

the proposed multi-objective scheme, the SIMP-PP scheme can be straightforwardly applied to other individual objective functions involving nonlinear or static and dynamic structures in the same manner. In fact both SIMP and PP can be successfully applied to both linear and non-linear problems.

According to PP multi-objective programming scheme, the problem formulation for compliant mechanisms can be expressed as follows:

$$\left\{ \begin{array}{l} \underset{X=(x_1, x_2, \dots, x_m)^T}{\text{Minimize}} : f_a(X) = \log_{10} \left\{ \frac{1}{n} \sum_{i=1}^n \bar{f}_i(f_i(X)) \right\} \\ \text{Subject to : } \left\{ \begin{array}{l} \sum_{j=1}^m x_j - V^* \leq 0 \\ 0 < x_{\min} \leq x_j \leq 1 \\ u_{in}(x)/u_{in}^* - 1 \leq 0 \end{array} \right. \end{array} \right. \quad (4)$$

X is the vector of the design variables and m is the number of elements in the mesh. $x_{\min}=0.0001$ is introduced to avoid singularity of the finite element procedure. $u_{in}(x)/u_{in}^* \leq 1$ is introduced to limit the allowable displacement at the input port in order to control the maximum stress level in the resulting mechanism. The aggregate objective function f_a is the representation of all the individual class functions. In this project it is the additional natural log operation discussed in Equation (2) and shown in Equation (4), where the aggregate objective is the log of the product between sum of the individual objectives and the inverse of the number of individual objectives.

To perform the design sensitivity analysis, a designer needs to find the relations between the aggregate objective function f_a and the design variables. f_a is dependent on the class functions \bar{f}_i , where i ($i = 1, 2, \dots, n$) represents the number of individual objective functions, \bar{f}_i is dependent on the individual objective functions f_1 and f_2 , and the objectives f_1 and f_2 are related to the design variable vector X . Thus, the design sensitivity of f_a with respect to design variable x_j ($j = 1, 2, \dots, m$) can be expressed as

$$\frac{\partial}{\partial x_j} [f_a(X)] = \sum_{i=1}^n \frac{\partial f_a}{\partial \bar{f}_i} \left(\frac{\partial \bar{f}_i(f_i(X))}{\partial f_i} \frac{\partial f_i}{\partial x_j} \right) = \frac{\partial f_a}{\partial \bar{f}_1} \left(\frac{\partial \bar{f}_1}{\partial f_1} \frac{\partial f_1}{\partial x_j} \right) + \frac{\partial f_a}{\partial \bar{f}_2} \left(\frac{\partial \bar{f}_2}{\partial f_2} \frac{\partial f_2}{\partial x_j} \right) \quad (5)$$

For example, considering Equation (2), we have

$$\frac{\partial}{\partial x_j}[f_a(X)] = \frac{2 \log_{10} e}{(\bar{f}_1(MSE) + \bar{f}_2(SE))} \left(\frac{\partial \bar{f}_1}{\partial(MSE)} \frac{\partial(MSE)}{\partial x_j} + \frac{\partial \bar{f}_2}{\partial(SE)} \frac{\partial(SE)}{\partial x_j} \right) \quad (6)$$

where e is the constant parameter of 2.71828.

The sensitivity terms $\partial \bar{f}_1 / \partial MSE$ and $\partial \bar{f}_2 / \partial SE$ denoting the class function \bar{f}_i with respect to the individual objective function f_i can be easily resolved by differentiating Equation (7) with respect to the f_1 (MSE) and f_2 (SE) on both sides, respectively

$$\begin{cases} (1) \bar{f}_i = (\lambda_i^k)^4 \left(\frac{a}{12} (\mu_i^k)^4 + \frac{b}{12} (\mu_i^k - 1)^4 \right) + c \lambda_i^k \mu_i^k + d, \text{ for } f_i > f_1^k; \\ \text{where } \lambda_i^k = \frac{f_i(X) - f_i^{k-1}}{f_i^k - f_i^{k-1}}, \mu_i^k = f(X)_i - f_i^{k-1} \\ (2) \bar{f}_i = \bar{f}_i^1 e^{\frac{s_i^1(f_i(X) - f_i^1)}{f_i^1}}, \text{ for } f_i \leq f_1^1; \end{cases} \quad (7)$$

Then, we can obtain the following design sensitivities

$$\frac{\partial \bar{f}_i}{\partial f_i} = \frac{4(f_i(X) - f_i^{k-1})^3}{3(f_i^k - f_i^{k-1})^4} \left[\frac{a(f_i^k - f_i^{k-1})^3}{b(f_i^k - f_i^{k-1} - 1)^3} + 2c \frac{f_i(X) - f_i^{k-1}}{f_i^k - f_i^{k-1}} + d \right], \text{ if } f_i > f_1^k \quad (8)$$

$$\frac{\partial \bar{f}_i}{\partial f_i} = \frac{\bar{f}_i^1 s_i^1}{f_i^1} e^{\frac{s_i^1(f_i(X) - f_i^1)}{f_i^1}}, \text{ if } f_i \leq f_1^1 \quad (9)$$

As shown in Figure 1. s is the slope of the objective function and a, b, c, d are constants introduced by Messac (Messac 1996), with k being the preference range at which the objective functions lie.

With finite element discretization and considering SIMP interpolation scheme, the objective functions SE and MSE and their design sensitivities are given as follows.

$$SE = \sum_{j=1}^m (E_{\min} + x_j^p \Delta E) \{u_{1,j}\}^T [k_j] \{u_{1,j}\} \quad (10)$$

$$\frac{\partial(SE)}{\partial x_j} = -\{U_1\}^T \left(\frac{\partial[K_1]}{\partial x_j} \right) \{U_1\} = -\sum_{j=1}^m p x_j^{p-1} \{u_{1,j}\}^T [k_j] \{u_{1,j}\} \Delta E \quad (11)$$

$$MSE = \sum_{j=1}^m (E_{\min} + x_j^p \Delta E) \{u_{2,j}\}^T [k_j] \{u_{1,j}\} \quad (12)$$

$$\frac{\partial(MSE)}{\partial x_j} = -\{U_2\}^T \frac{\partial[K_2]}{\partial x} \{U_1\} = -\sum_{j=1}^m p x_j^{p-1} \{u_{2,j}\}^T [k_j] \{u_{1,j}\} \quad (13)$$

Where $\Delta E = E_0 - E_{\min}$, $\{U_1\}$ is the global displacement field corresponding to the actually applied force F_{in} at the input port as illustrated in Figure 3, $\{U_2\}$ is the global displacement field caused by the dummy load F_d applied at the output port as shown in Figure 4, $[K_1]$ and $[K_2]$ are the global stiffness matrices of the structure including and excluding the output spring k_s respectively. The variables $u_{1,j}$, and $u_{2,j}$ are the element displacement fields of the j^{th} element that constitute $\{U_1\}$, and $\{U_2\}$ respectively. While similarly k_j is the element stiffness matrix of the j^{th} element.

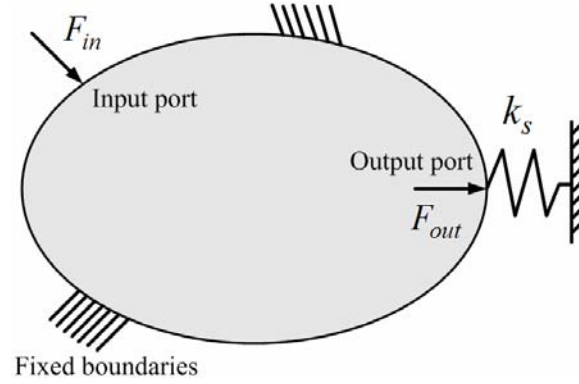


Figure 3 Structural SE

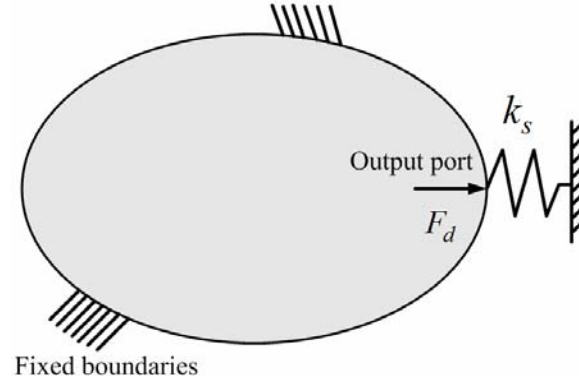


Figure 4 Mechanical MSE

2.4 Numerical examples of using SIMP-PP in structural design

To demonstrate the feasibility of SIMP-PP in the multi-objective topology optimization of compliant mechanisms, this section provides two widely studied examples to compare and

demonstrate its capabilities against the single objective SIMP optimization, namely the compliant force inverter and the compliant gripper.

2.4.1 Compliant inverter

Figure 5 illustrates the compliant inverter problem. The design domain is a square region meshed with 100×100 quad4 finite elements in a $100 \mu m \times 100 \mu m$ domain. The mechanism is fixed at its top left and bottom left corners and its functionality is to provide motion in the $+x$ direction at its output port up on an actuation force of $-20 \mu N$. The contact between the output port and the unspecified work piece is represented as a spring with spring stiffness k_s of $10 N/m$. The material of interest is polycarbonate polymer with elastic modulus of $1.5 GPa$ and has a Poisson ratio of 0.31 . The material volume constraint is limited to no more than 25% of the total volume of the design domain, however this is implemented in the classic SIMP approach rather than the PP approach as class 1-H as both schemes would suffice, but the original formulation is more compatible when OC or MMA is applied.

The multi-criteria objectives in this problem are to minimize the strain energy of the system to achieve stiffness and to maximize the displacement at the output port for greater performance. The problem statement is written as maximizing displacement (class 2-S) and minimizing SE (class 1-S). The preferences are constructed with the following hypothetical design information: it would be highly desirable to achieve an output displacement of more than $0.8 \mu m$, while the minimum performance requirement of $0.3 \mu m$ should not be compromised. As with regards to strain energy, based on experience they should be maintained between $1 e-6 \mu J$ to $4 e-6 \mu J$.

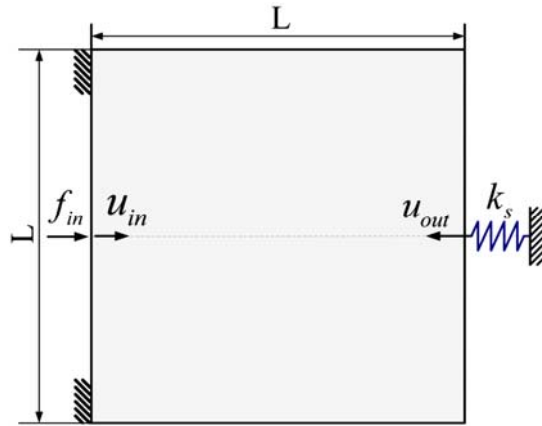


Figure 5 Design domain of the compliant inverter

This example reflects the flexibility of PP through the selection of objective functions with non-identical physical qualities (joules and meters) and at several orders of magnitudes apart ($1e-6$); in this problem the ranges of preferences are based on the design requirement and also the designer's preference. When applying SIMP-PP to the design of compliant airfoil structures the objective functions can easily be changed to more relevant subjects such as; maximize tip deflection angle of the airfoil structure, while minimize deformation/SE under aerodynamic loading. Multiple optimizations were conducted under various displacement preferences to illustrate the flexibility of SIMP-PP in reflecting the designer's preference in linear and non-linear fashion. Effect of preference assignment on the solution in terms of both topology and performance are investigated.

The articulation of preferences in each case is as follows. In case *d* both design preferences are assigned based on linear interpolation of their design requirement, in the remaining cases the design focus is shifted by altering the displacement preference range to reflect the designers changing desirability to achieve large output displacement (while holding the strain energy preferences constant as in case *d*), with cases *a* and *g* acting as the two extremities. This is done by assigning the displacement preferences to be either very high or very low (effectively becoming single objective optimizations of displacement output, and mean compliance). Other cases represent a transition from one extremity to another as shown in Figure 6.

The optimization results for the compliant force inverter are presented below; Figure 7 includes the optimal topologies, while Table 3 illustrates a qualitative visualization of the optimization procedure. Table 4 shows the objective functions summary. Figure 8 displays the convergence process and Figure 9 shows the Pareto front generated.

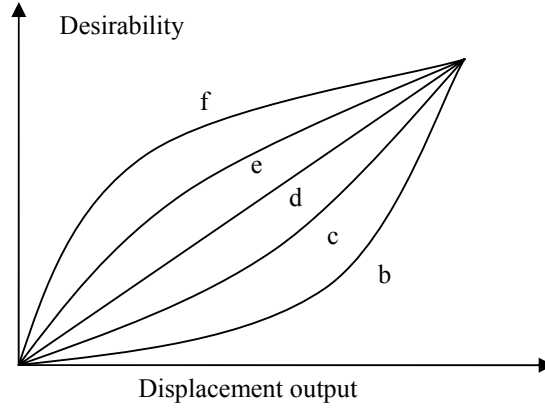


Figure 6 Shift in desirability for large displacement output in cases b to f

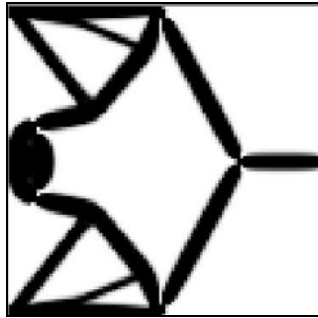
Table 3 SIMP-PP optimization results for compliant force inverter

Case	Operation	Highly Des.	Desirable	Tolerable	Undesirable	Highly Undes.
		f_{i1}	f_{i2}	f_{i3}	f_{i4}	f_{i5}
a	maximize output (μm)	$+\infty$	$+\infty$	$+\infty$	$+\infty$	$+\infty$
	minimize SE ($1\text{e-}6\mu\text{J}$)	1	1.75	2.5	3.25	4
b	maximize output (μm)	0.8	0.7688	0.675	0.5188	0.3
	minimize SE ($1\text{e-}6\mu\text{J}$)	1	1.75	2.5	3.25	4
c	maximize output (μm)	0.8	0.75	0.65	0.5	0.3
	minimize SE ($1\text{e-}6\mu\text{J}$)	1	1.75	2.5	3.25	4
d	maximize output (μm)	0.8	0.675	0.55	0.425	0.3
	minimize SE ($1\text{e-}6\mu\text{J}$)	1	1.75	2.5	3.25	4
e	maximize output (μm)	0.8	0.6	0.45	0.35	0.3
	minimize SE ($1\text{e-}6\mu\text{J}$)	1	1.75	2.5	3.25	4
f	maximize output (μm)	0.8	0.5813	0.425	0.3312	0.3
	minimize SE ($1\text{e-}6\mu\text{J}$)	1	1.75	2.5	3.25	4
g	maximize output (μm)	≈ 0	≈ 0	≈ 0	≈ 0	≈ 0
	minimize SE ($1\text{e-}6\mu\text{J}$)	1	1.75	2.5	3.25	4

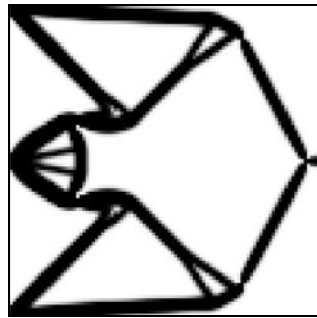
Table 4 Objective function summary

<i>Case</i>	<i>SE (1e-6μJ)</i>	<i>Output (μm)</i>
<i>a</i>	3.741	0.770
<i>b</i>	3.157	0.544
<i>c</i>	3.072	0.496
<i>d</i>	2.945	0.483
<i>e</i>	2.917	0.458
<i>f</i>	2.829	0.441
<i>g</i>	1.215	0

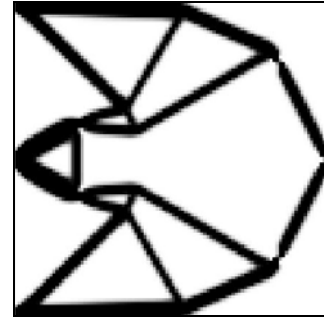
Table 3 shows SIMP-PP produces solutions with fairly balanced degree of desirability between the two objective functions, with the exception of cases *a* and *g* due to the extremity in their articulation of preferences. This is due to the formulations in Equation (2) and Equation (3) which implicitly causes the least desirable objective function to dominate the optimization process. This can be seen as an advantage for real engineering designs as it assists in avoiding unrealistic solutions which provide numerically sound overall performance but large discrepancies in balancing each individual criterion. The numerical results are shown in Table 4, from which the maximum output the inverter can achieve is $0.77 \mu\text{m}$ while incurring a SE of $3.741e-6\mu\text{J}$.



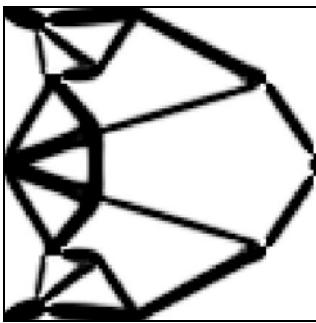
(a)



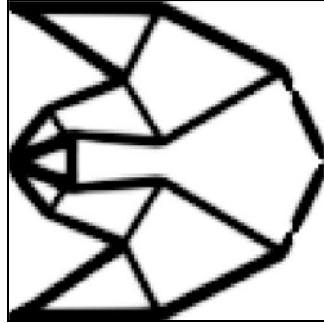
(b)



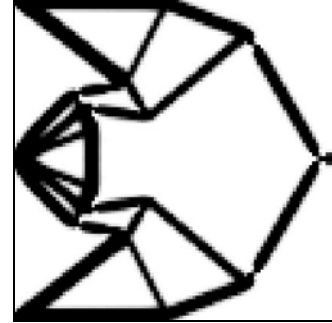
(c)



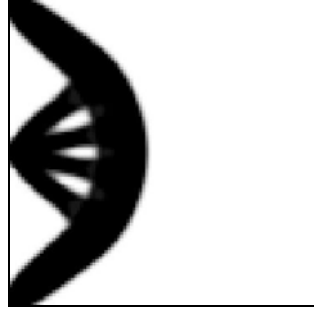
(d)



(e)



(f)



(g)

Figure 7 Compliant inverter topologies under various design priorities

Figure 7 shows the effect of altering the priority or the desirability of displacement output on the topology, the preferences are assigned to reflect a high priority for large displacement in case *a*, and a gradual shift in focus throughout each case. The effect on the topology is most evident at the input port, where it transformed from a solid lump of material (case *a*) to a high density truss structure (case *g*). In case *g* the optimization effectively becomes a mean compliance problem and the numerical effect relating to the displacement objective was effectively ignored in the optimization procedure, thus the resulting topology in Figure 7g has no structural links to the output port, but rather concentrated near the loading point.

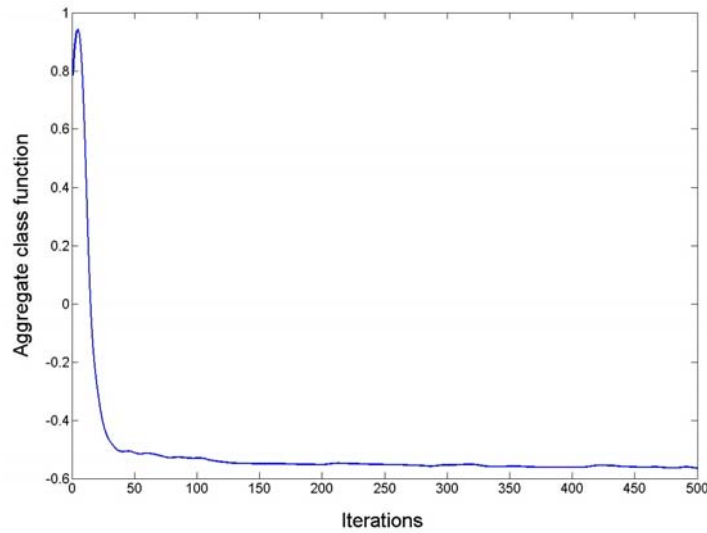


Figure 8 Typical convergence history for compliant inverter

Figure 8 displays the convergence history for this problem. The figure displays convergence up to 500 iterations, but in fact convergence is usually achieved within 300 iterations under a convergence factor of 1%, hence the run time and the number of iterations in SIMP-PP is

comparable to a SIMP run, however it may take longer in cases of an unrealistic preference range such as in case *a* and *g*. Setting wildly demanding preference ranges could harm the stability of the convergence, while setting preferences too generously could cause slow realization of topology. These can be largely avoided by exercising reasonable judgment on preference assignments. The numerical stability of SIMP-PP is one area further research is required. From experience the chances of termination due to numerical instability are truly rare, and thankfully it happens in the early stages of the iteration which allows the designers to rectify and commence a re-run quickly. The instability arises not in PP nor SIMP but the converging nature of the global convergence procedure in the optimization; in some occasions the optimization experiences large oscillations in the design variable matrix during its initial stage, and for certain objectives this could possibly translates to a sharp jump of several magnitudes, the class function (due to its fourth order nature) further amplifies the value and also its derivative, resulting in computational instability. For now the stability issue is assisted by initialize the SIMP-PP mesh with a partially converged mesh from a previous run and also setting upper limits to the sensitivity values. The Pareto front is shown in Figure 9; it is shown to be almost linear with a slight degree of convex function.

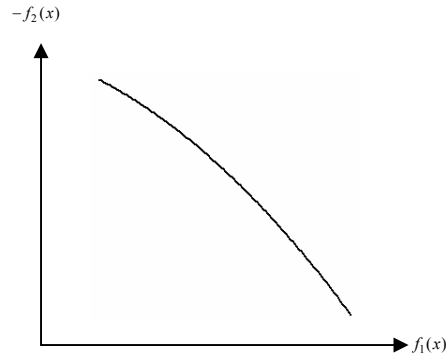


Figure 9 Pareto front generated by SIMP-PP

2.4.2 Compliant gripper

The sketch in Figure 10 illustrates the design problem for a micro compliant gripper. Upon actuation by an input force of $20\mu N$ the gripper would shut and clamp on to the work subject placed in the void region. The design domain is of identical size and mesh to the previous example, with an additional pre-defined void region (passive design region) between the

grips. The performance aspects are to ensure the gripper has sufficient vertical displacement for the gripping function under certain artificial spring which characterizes the contact condition, and secondly has sufficient stiffness. The design constraint is to confine the material usage to 25% of the entire domain volume. The hypothetical design requirement for the compliant gripper is described as: it would be highly desirable to achieve a vertical displacement of more than $0.6\mu\text{m}$, while the minimum requirement is roughly $0.1\mu\text{m}$. Based on experience the strain energy should be maintained between $1\text{e-}6\text{ }\mu\text{J}$ to $3.5\text{e-}6\text{ }\mu\text{J}$.

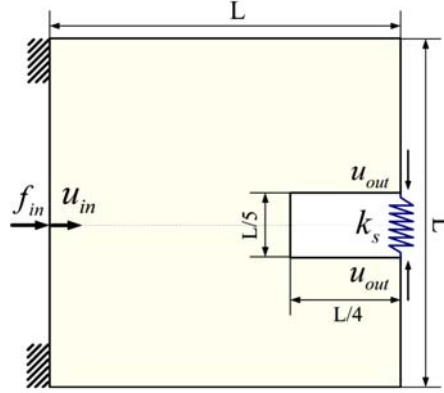


Figure 10 Design domain of compliant gripper

The articulations of preferences are conducted in similar fashion to case *d* in the force inverter example, which is partially based on the design information given above and partially on the designers' preference. In this example the influence of the artificial spring at the output port is investigated by using various spring constants (evenly spaced between 10 to 40 N/m) while holding the preferences constant. The optimization results for the compliant gripper are shown in the following section; Figure **11** includes the optimal topologies, while Tables **5** and **6** showcase the qualitative visualization of the optimization procedure and the objective functions summary respectively.

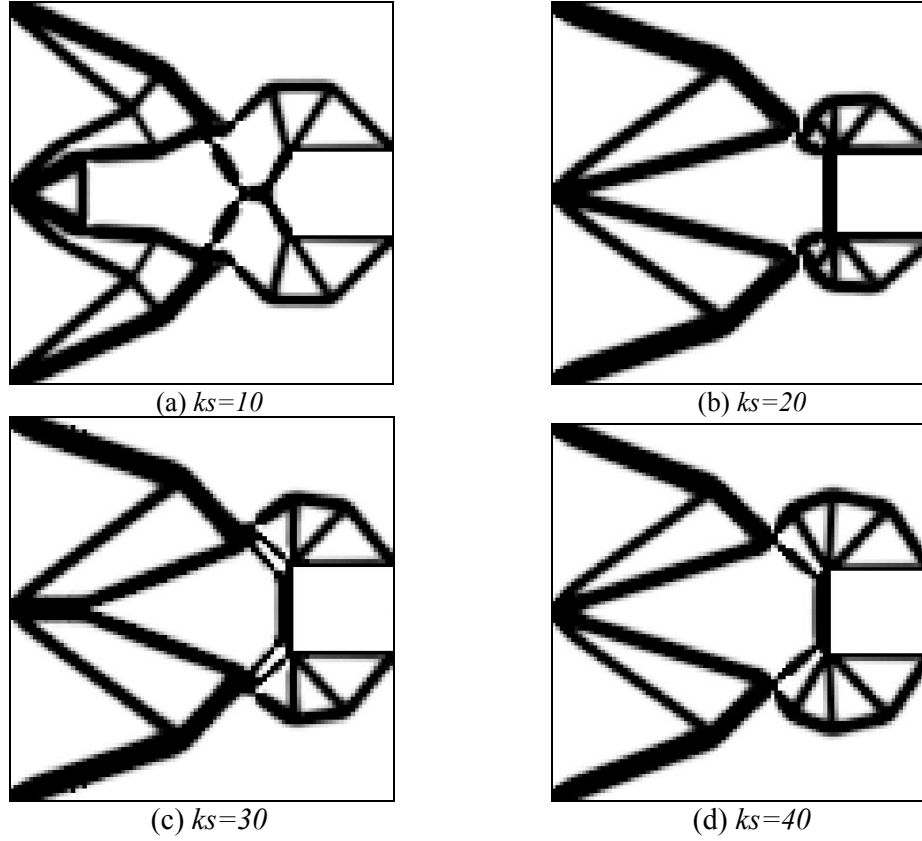


Figure 11 Topology layouts for compliant gripper under different ks

Table 5 SIMP-PP optimization results for compliant gripper

Case	Operation	Highly Des.	Desirable	Tolerable	Undesirable	Highly Undes.
		f_{i1}	f_{i2}	f_{i3}	f_{i4}	f_{i5}
a	maximize output (μm)	0.6	0.475	0.35	0.225	0.1
	Minimize SE ($1e-6\mu J$)	1	1.625	2.25	2.875	3.5
b	maximize output (μm)	0.6	0.475	0.35	0.225	0.1
	Minimize SE ($1e-6\mu J$)	1	1.625	2.25	2.875	3.5
c	maximize output (μm)	0.6	0.475	0.35	0.225	0.1
	Minimize SE ($1e-6\mu J$)	1	1.625	2.25	2.875	3.5
d	maximize output (μm)	0.6	0.475	0.35	0.225	0.1
	Minimize SE ($1e-6\mu J$)	1	1.625	2.25	2.875	3.5

Table 6 Objective function summary for compliant gripper

<i>Case</i>	<i>SE (1e-6μJ)</i>	<i>Output (μm)</i>
<i>a</i>	2.638	0.405
<i>b</i>	2.749	0.202
<i>c</i>	2.912	0.185
<i>d</i>	3.091	0.177

From the results it is evident that the magnitude of ks has a noticeable impact on both the topology layout and the structural performance. Firstly on the topology, the increase in ks represents a harder work piece, thus the compliant gripper must also enhance its own structural stiffness to avoid any unwanted deformation of its own upon contact with the work piece. Evidently this is shown in Figure 11 with the gradual formation of large truss networks at the grip region. Secondly with respect to structural performance, the output displacement has been decreasing in exponential decay fashion with respect to the increase in ks . An interesting feature to note is that the SE have also increased, this is due to the build up of local deformation in the gripping process as a result of ks . This phenomenon is illustrated in Figure 12 with the comparison of strain energy contours in FEA software Strand7 using identical contour range, the figures show in case d there is a large region of high strain energy area around the mouth of the gripper, and the average strain energy in the base (aft portion) of the gripper is in case d generally higher than in case a . The FEA also validated the accuracy of the optimization procedure (linear model with quad4 elements) with solutions exhibiting roughly 8% to 11% discrepancy, which is most likely due to the rounding off of design variables in the FEA software.

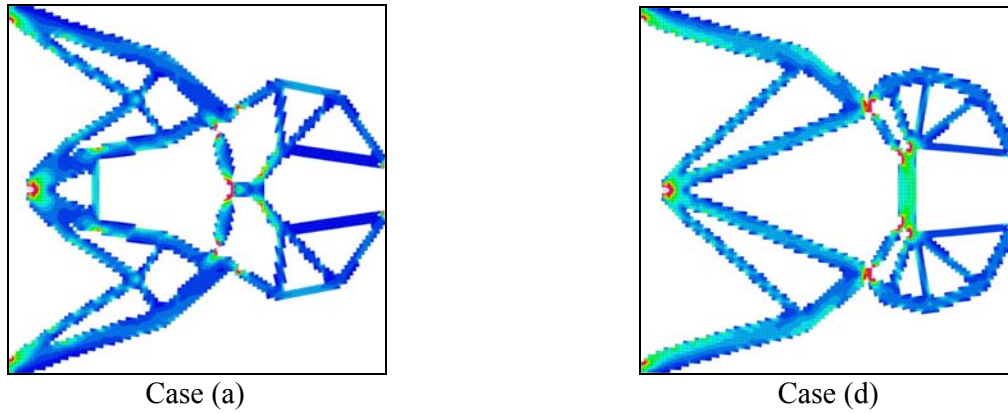


Figure 12 Strain energy contour due to deformation of cases a and d

Overall, the examples provided show that compliant mechanisms with multi-objectives can be meaningfully and simultaneously optimized with SIMP-PP. The objectives can consist of different physical qualities, different magnitudes, different optimization operations and linear/nonlinear degree of desirability.

3 Design of sandwich core architecture for shape morphing

3.1 *Modeling and design of single unit cell*

This section shall provide our explanation on some of the modeling aspects of the design directly related to compliant airfoil structures. We propose to base the optimization on a bi-material design, where there are two types of materials, one passive and one active with the active material severing as the actuation source when an external stimulus is applied. Trials have shown that bi-material design offers better performance than the single material design; this is mostly due to the fact that bi-material design takes advantage of the different material properties and enables unimorph configuration, which is naturally suited for structural deflection. The external stimulus for the active material can be of thermal, electrical or other physical systems; Hence the thermal actuation has been used to illustrate the concept.

The issue of wing skin is excluded from this study; the nature of adaptive wing causes several problems on the wing skin, such as the ability to achieve a suitable balance between stiffness and flexibility, and the ability to form a gapless skin over a deforming geometry. Hence this issue is as much as a material issue as a design issue; no current engineering material, both plastic and metallic is capable of providing such capabilities, and some of the leading candidates such as electro active polymer, certain silicone elastomer, and corrugated composites are still in the research phase.

3.1.1 *Design criteria*

The design objective in this problem is two fold, on one hand the unit cell must act compliant under the internal actuation by achieving substantial deflection, while on the other hand act stiff in resisting externally applied loads. Thus the topology optimization must be of multi-objective nature, in this case there are two individual objective functions, one is to maximize the difference in output displacement at output port 1 and 2 to implicitly maximize deflection angle, the other objective function is to minimize the strain energy (SE) of the structure under aerodynamic loading.

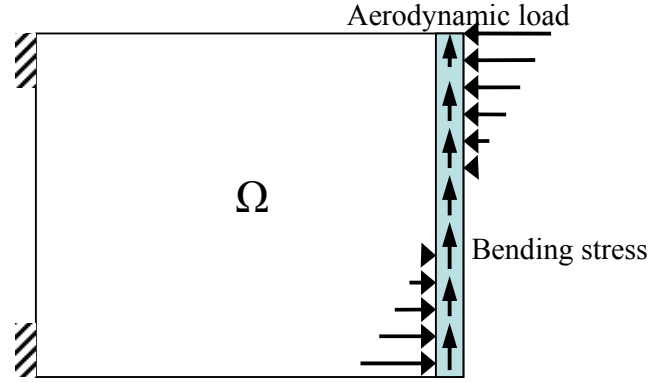


Figure 13 Strain energy criterion

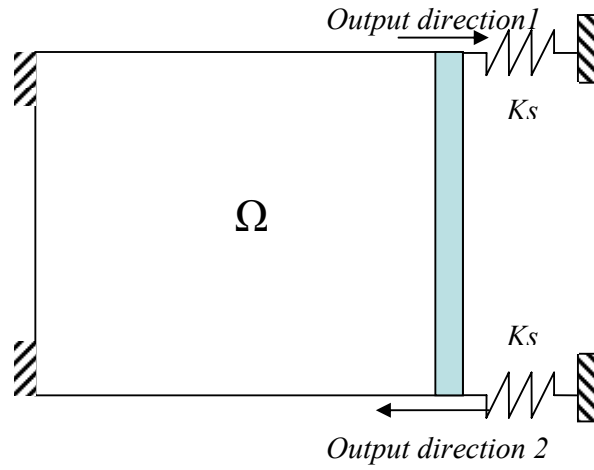


Figure 14 Deflection angle criterion

3.1.2 Loading conditions

The loading conditions on the unit cell are the aerodynamic loading transferred to the unit cell structure through the wing skin, and the accompanying bending stress which is counter productive to deflection transmitted through the adjacent cell. They are modeled as an evenly distributed vertical force and a linearly distributed horizontal force respectively.

3.1.3 Boundary conditions and connectivity conditions

The unit cell network in this case is chosen to be in series, with each cell linked behind another starting with the first unit cell at the trailing edge of the airfoil (eg >70% chord) and attached to a fixed spar. Thus the boundary condition is implemented by fixing the left edge of the design domain. The connectivity condition is implicitly implemented by defining a column of solid material at each cell wall that connects the current cell with the following one. The solid material region is to enforce the structural integrity at the edge where the next cell is connected to prevent local deformation, thus avoid unwanted deformation in the unit cell network.

3.1.4 Material interpolation

As there are effectively three types of solid phases in this bi-material design, two material types, and void. It is necessary to interpolate between the three phases during the optimization procedure so that the correct effective material properties such as elastic modulus E , and thermal expansion coefficient α are used in the solving of governing equations. Therefore by modifying Equation (1) to incorporate material two, a second design variable is introduced as shown in Equation (14)

$$E(x, v) = E_{\min} + v^p \left(x^p (E_1 - E_{\min}) + (1-x)^p (E_2 - E_{\min}) \right) \quad (14)$$

x is the design variable responsible for the interpolation between one solid material and the other, while v is the design variable responsible for the interpolation between solid and void material.

Due to the thermal-mechanical coupling of the compliant unit cell structure, the thermal properties will need to be interpolated in similar fashion, thus the effective thermal expansion coefficient of the two materials are shown in Equation (15)

$$\alpha(x) = \alpha_{\min} + x^p (\alpha_1 - \alpha_{\min}) + (1-x)^p (\alpha_2 - \alpha_{\min}) \quad (15)$$

In this part the effects of active material volume on the resulting structural layout and its performance are analyzed. The specified passive material is chosen as titanium, while the active material is Nitinol and its volume fractions are 5%, 7.5%, and 10% of the total design domain. The artificial stiffness implemented at the top and bottom right hand side edge is both 15 N/mm in the x direction.

3.1.5 Objective function and sensitivity analysis

With finite element discretization and the implementation of SIMP scheme, the objective function to describe the displacement criterion and the strain energy criterion u_{out1} , u_{out2} and SE are given as follows.

$$\begin{aligned} SE &= \sum_{j=1}^m (E_{\min} + x_j^p \Delta E) \{u_{1,j}\}^T [k_j] \{u_{1,j}\} \\ u_{out1} &= L_1^T U \\ u_{out2} &= L_2^T U \end{aligned} \quad (16)$$

Where $u_{1,j}$ and k_j are the element displacement vector and element stiffness matrix, L_1 and L_2 are zero vectors with a single 1 at the row number corresponding to the degree of freedom of the output port u_{out1} and u_{out2} respectively. Since the strain energy sensitivity equations were discussed in detail previously, here we will only emphasis on the displacement equations. The adjoint sensitivity analysis is applied in the displacement design objective, due to its high computational efficiency in situations with large number of design variables and few number of design functions. The analysis is carried out in the following section with u_{out2} sharing the same procedure.

$$\begin{aligned} \text{mechanical} : K_I(x, v) U_I(x, v) &= F_I(U_{II}(x, v), x, v) \\ \text{thermal} : K_{II}(x, v) U_{II}(x, v) &= F_{II} \end{aligned} \quad (17)$$

The displacement caused by the actuation is a result of thermal-mechanical coupling; therefore the analysis will need to incorporate both the mechanical response and the thermal response of the system. In Equation (17), the sub index I represents the mechanical system while II represents the thermal system. K_I , U_I and F_I are the global stiffness matrix, global displacement field and global force field. K_{II} , U_{II} and F_{II} are the thermal conductivity matrix, temperature field and thermal load vector.

The equations in (17) can easily be solved in finite element analysis given the appropriate loading conditions, and assuming the system is linear the displacement expression in (16) can be re-written as Equation (18), with λ_1 and λ_2 as adjoint vectors with same length as the displacement field.

$$\begin{aligned} u_{out1} &= L_1^T U_I(x, v) + \lambda_{1,I}^T (F_I(U_{II}(x, v), x, v) - K_I(x, v) U_I(x, v)) \\ &\quad + \lambda_{2,I}^T (F_{II} - K_{II}(x, v) U_{II}(x, v)) \end{aligned} \quad (18)$$

The sensitivity of the output displacement with respect to either the x or v variable can therefore be expressed as follows.

$$\begin{aligned} \frac{\partial u_{out1}}{\partial x} = & L_1^T \frac{\partial U_I(x, v)}{\partial x} + \lambda_{1,I}^T \left(\frac{\partial F_I(U_{II}(x, v), x, v)}{\partial x} - \frac{\partial K_I(x, v)}{\partial x} U_I(x, v) - \frac{\partial U_I(x, v)}{\partial x} K_I(x, v) \right) \\ & + \lambda_{1,II}^T \left(-\frac{\partial K_{II}(x, v)}{\partial x} U_{II}(x, v) - \frac{\partial U_{II}(x, v)}{\partial x} K_{II}(x, v) \right) \end{aligned} \quad (19)$$

To solve the sensitivity, all the $\frac{\partial U}{\partial x}$ terms on the left hand side of Equation (19) should cancel.

To achieve this following conditions are implemented by selecting the appropriate values for the adjoint vectors as in Equation (20)

$$\begin{aligned} L_1 &= \lambda_{1,I} K(x, v) \\ \lambda_{1,I} \frac{\partial F_I(U_{II}(x, v), x, v)}{\partial x} &= \lambda_{1,II} K_{II}(x, v) \end{aligned} \quad (20)$$

Therefore the final sensitivity equation of the displacement output with respect to the design variable x is given by Equation (21). The sensitivity of the displacement output with respect to design variable v can be analyzed in the same fashion without any conceptual difficulties and the same applies to u_{out2} .

$$\frac{\partial u_{out1}}{\partial x} = \lambda_{1,I}^T \left(-\frac{\partial K_I(x, v)}{\partial x} U_I(x, v) \right) + \lambda_{1,II}^T \left(-\frac{\partial K_{II}(x, v)}{\partial x} U_{II}(x, v) \right) \quad (21)$$

3.1.6 Remarks

Regarding the continuum-type topology optimization, the relaxed optimization problem with SIMP scheme is prone to numerical instabilities in general, and density filtering technique is used to smear out the mesh-dependency and checkerboards.

It is well known that the formulation given in Equation (4) is for large-scale optimization problems with non-convex objective functions and multiple constraints. When it comes to selection of the appropriate convergence algorithm, the theoretically well-founded mathematical programming algorithms are somewhat more efficient and flexible in dealing with such optimization problems. In particular, the method of moving asymptotes (MMA) (Svanberg 2002) belonging to sequential convex programming is currently regarded as one of the most robust optimization algorithms for solving advanced topology optimization

problems. Using concept of convex separable approximations the MMA scheme transfers the original optimization problem into a sequence of linearized, strictly convex and separable sub-problems, however, it is noted that the MMA method does not guarantee the global optimal point due to non-convexity of the original optimization (Svanberg 1995).

3.1.7 An illustrative example

This example illustrates the design of a compliant unit cell capable of edge deflection through topology optimization. The domain is a size 100 x 100 mm square plate with 1mm thickness, meshed using 10000 quad4 elements. A uniform thermal temperature of 10°C is applied to the domain (excluding the fixed region) as the actuation for the deflection of the passive edge located at the right hand side of the unit cell, the deflection is implicitly mathematically expressed using the difference in the horizontal displacement of the edge at two different locations. The loading condition and boundary conditions are similar to that of Figure 13 and Figure 14 with artificial loading scenarios. The design domain is shown in Figure 15.

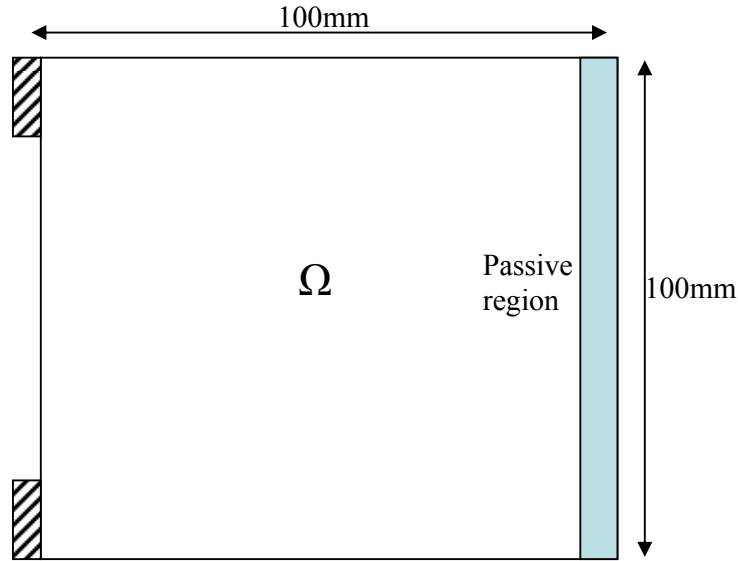


Figure 15 Design domain of the compliant unit cell

The topologies in Figure 16 and Figure 17 show the different topologies arrived by altering the amount of active material available for usage. The red region represents the active material, which is the SMA material that is mechanically sensitive to thermal actuation,

while the green region represents the passive material. Two different types of artificial passive materials are presented, one of which has a high elastic modulus comparative to the active material (Nitinol, $E = 75\text{GPa}$, $\nu = 0.31$), the other is of a weaker modulus. The results are generated by the finite element software Strand7.

From Figure 16 and Figure 17, it is observed that each unit cell exhibits a mixed degree of tension and unimorph actuation mechanism, which is a result of bi-material structural composition. The edge deflection of the unit cell was larger under the passive structure with the higher elastic modulus; this is due to the stiff boundary condition implemented at the output port, which is indicated by the presence of significant unimorph mechanism at the cell edge displayed in Figure 17. Table 8 summarizes the deflection angle and the horizontal displacement at the two output locations for each case. As expected, greater Nitinol content contributed to a larger deflection angle, however the resulting increase in deflection angle may not be proportional to the added Nitinol content.

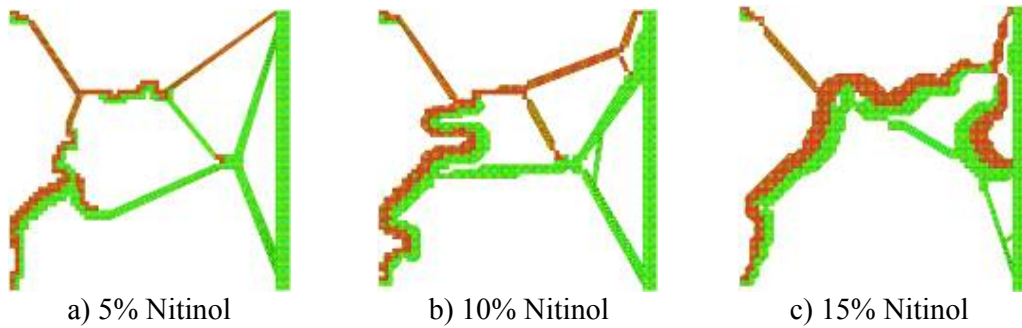


Figure 16 Topologies with varying Nitinol content with strong passive material

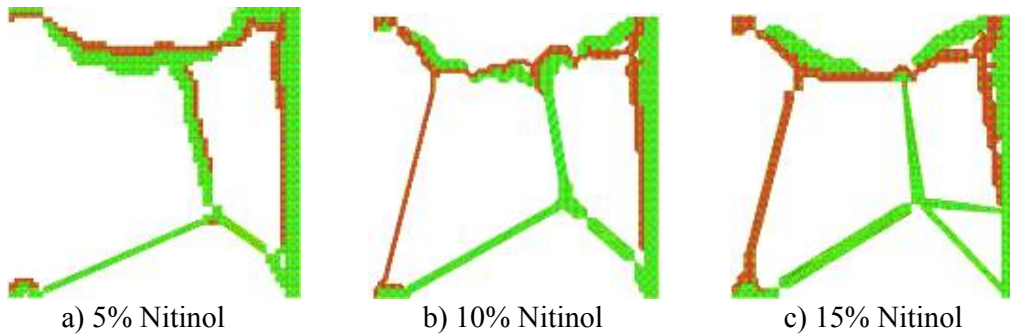


Figure 17 Topologies with varying Nitinol content with weak passive material

Table 7 Data for optimal topology with varying volume fractions

Case	U_{out}^1 (mm)	U_{out}^2 (mm)	Deflection (deg)
A	4.42	-4.67	8.75
B	5.17	-5.96	10.75
C	7.20	-7.87	14.71
D	3.04	-3.81	6.56
E	3.97	-4.58	8.21
F	4.58	-4.68	8.91

3.2 Assembling of multiple unit cells

In this part the effect of combining multiple unit cells in series is analyzed, the structural layout is taken from one of the topologies, and had its features refined in FEA before analysis. The purpose of refining its features is to enhance its manufacturing ease, by removing hinges, smoothing its contour, and refining its mesh in stress concentrated and sharp curvature areas. Below shows the structures composing 1, 2 and 3 unit cells both before and after actuation.

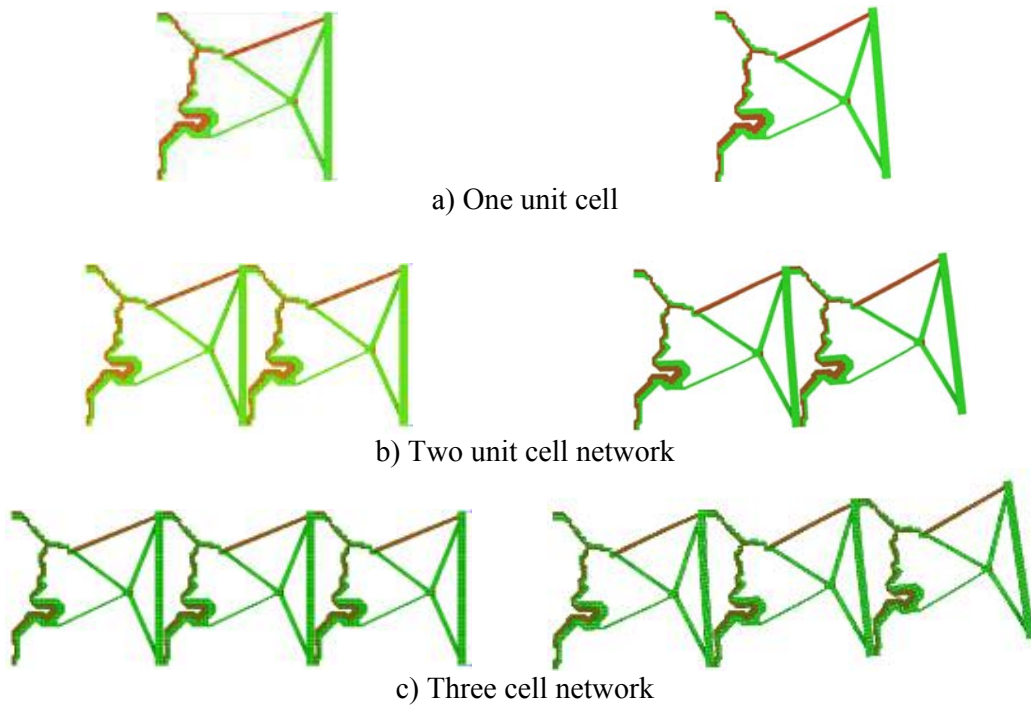


Figure 18 Performance of different unit cell networks before (left) and after (right) actuation

Table 8 and Figure 19 display the data for deflection angle versus number of cells for up to six cells. The analysis was conducted in Strand7 under linear static condition. The results indicate that the deflection increment decreases with each increase in the number of cells.

Table 8 Data for deflection angle with varying number of unit cells

Number of cells	Edge deflection angle(deg)
1	4.83
2	7.16
3	8.56
4	9.46
5	10.19
6	10.69

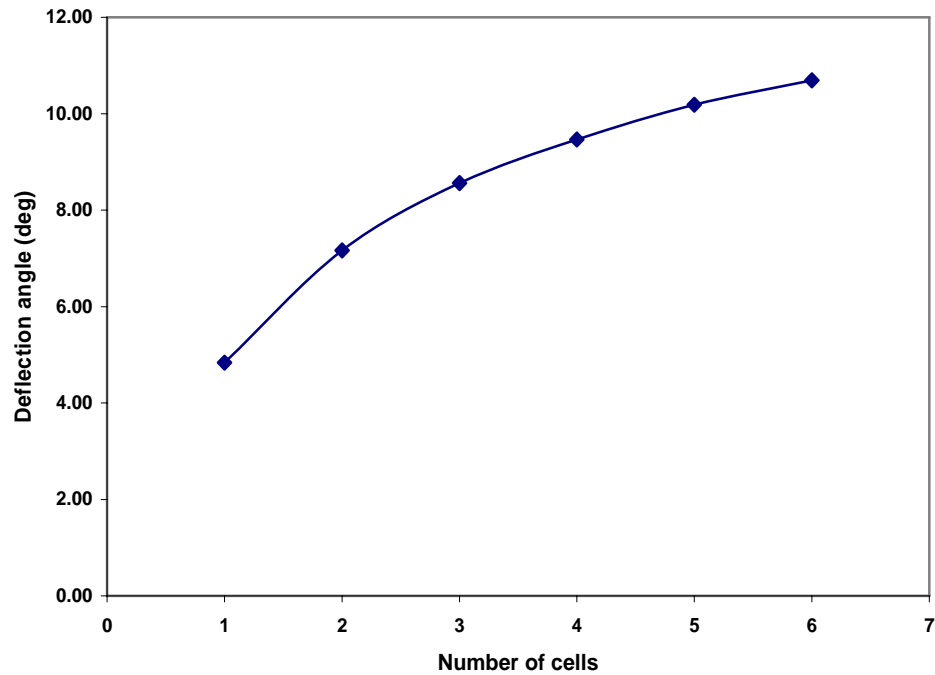


Figure 19 Plot of deflection angle vs number of cells

4 Demonstrative testing

4.1 Post processing and prototyping

The main principle of interest in the prototyping of the compliant airfoil structure is to validate the design approach of using topology optimization of unit cell structures in the synthesis of compliant airfoil structures.

To transform the two dimensional topology into a three dimensional design that can be tested in laboratory condition, it is necessary to post-process the raw topology into a design that is practical and applicable. The process sequence by which the final design is arrive is shown in Figure 20.

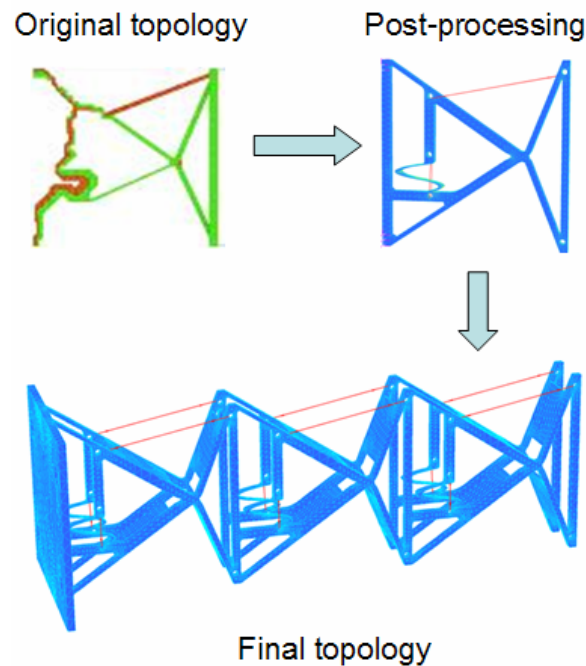


Figure 20 Stages of post-processing

First the topology is transformed into FEA software Strand7 to remove the mechanical hinge like structures into flexible pivots. The so called “hinges” refers to single point pivots that connect the structure together while providing little resistance to rotation; the hinges represent arguably mechanical pivots which violate what constitutes a compliant mechanism. Subsequent post processing involves identifying the deflection mechanisms in the structure,

such as unimorph characteristics and tension characteristics, and modifies the topology in areas that are necessary with regards to fabrication capability while maintain the original deflection mechanisms. Modifications are also made under material considerations, Eventually the topology is extruded in its thickness direction to fully realize a three dimensional structure, without the extrusion the structure is susceptible to out of plane buckling and would lack the lateral stability for demonstrative testing.

The prototype is made by rapid prototyping form Fused Deposition Modeling; in which the model is built based on its cross section profile supplied from specific computer aided design (CAD) package by using an extrusion nozzle to direct the specific molten material into the co-ordinate of the material occupying region. The material hardens immediately after exiting the nozzle and the model is built as each slice is added to the previous one.

The active material is implemented using commercially available Nitinol springs designed to be driven by joule's heating, and is attached to the passive structure through screws as shown in Figure 21.

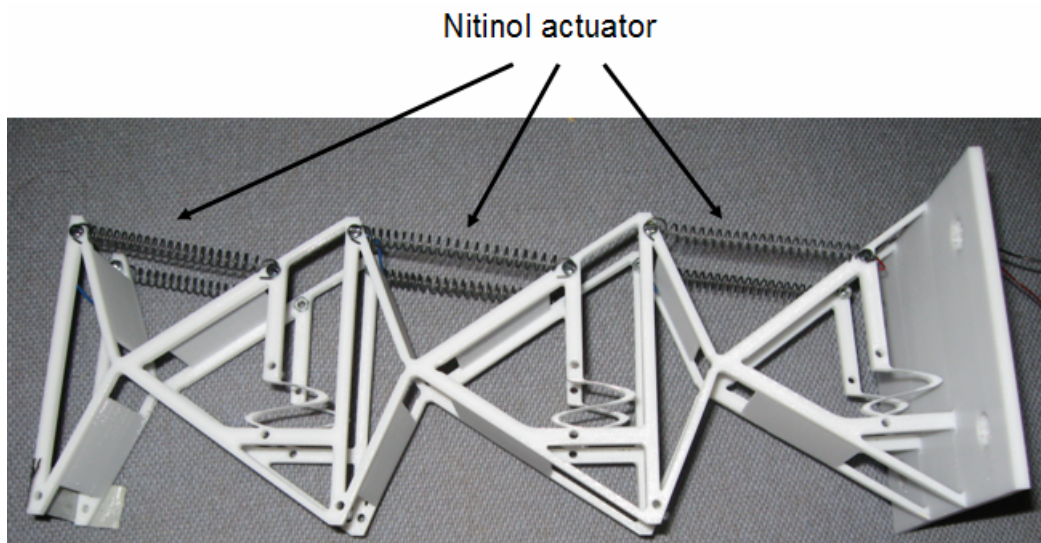


Figure 21 Final prototype product of 3 cells compliant network

4.2 Experiment

4.2.1 Test set-up

The main purpose of the experiment is to demonstrate the feasibility of the design, with the main parameter of interest being the deflection angle. The experiment is controlled by passing a known current through the Nitinol springs to cause Joule's heating, and through attached sensors connected to a data-logging system, the thermal-mechanical characteristics of the active material in terms of temperature, voltage, and the resulting actuation force can be controlled. The setup of the actuation system is shown in Figure 22.

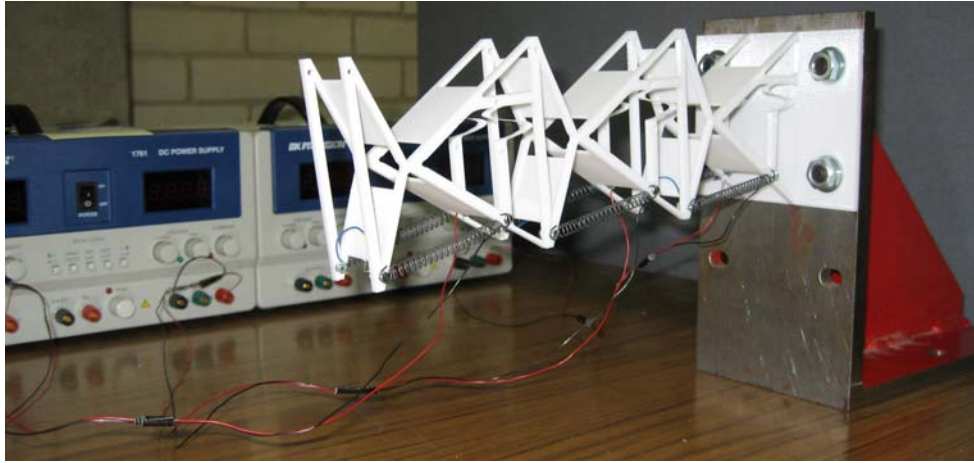
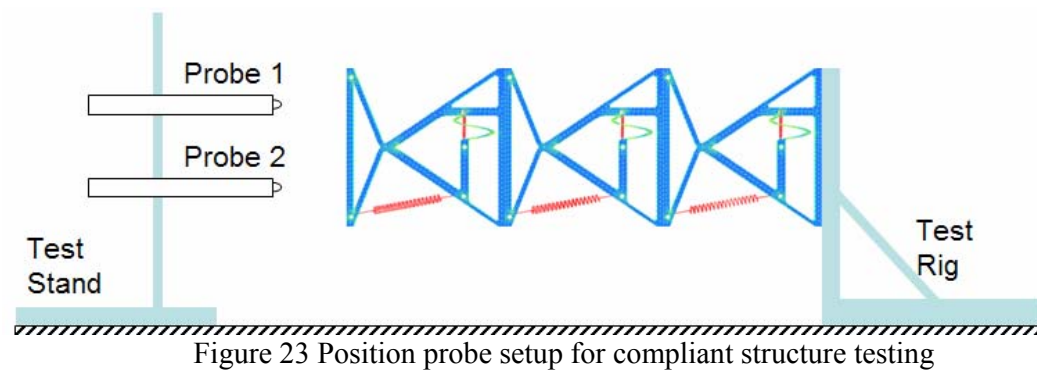


Figure 22 Test setup of 3 cell compliant network

The structure subjected to testing is a 3 cell structure with each cell occupying a volume of $100\text{mm} \times 100\text{mm} \times 45\text{mm}$. Each cell is actuated by two Nitinol spring actuators with spring constant capacity of 220N/m at martensite phase with austenite-martensite transition temperature at around 43°C . The transition is triggered by joule's heating under constant 0.6A power supply. The deflection angle is measured by a pair of position sensors placed opposite to the compliant structure as shown in Figure 23, the sensors are placed a known vertical distance apart and measures the horizontal displacement movement at the cell wall; due to the fact that the cell wall remains locally un-deformed during the actuation the deflection angle can be measured with accuracy based on the position measurements. The Nitinol response to Joules heating in terms of temperature and voltage are also tracked during the experiment.



4.2.2 Results and discussion

The results below in Figure 24-Figure 28 illustrate the behavior of some of the key parameters of interest for this experiment. Subsequent discussions related to the parameters are presented in the following.

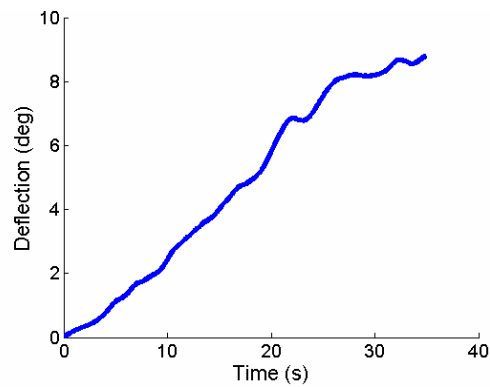


Figure 24 Tip deflection angle under 0.6A actuation vs time

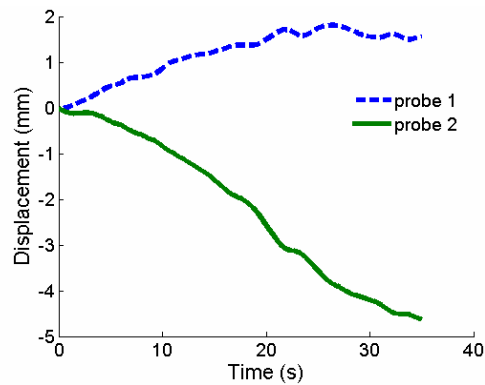


Figure 25 Horizontal position movements of cell wall vs time

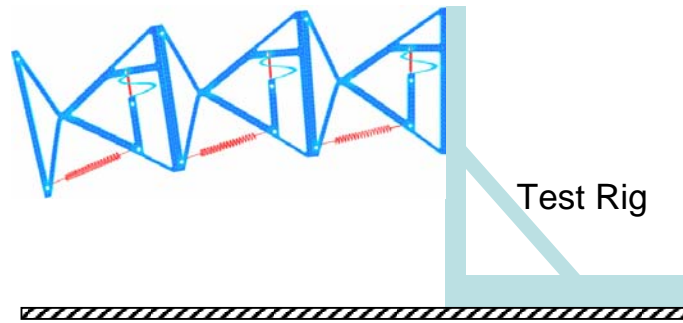


Figure 26 Graphic illustration of deflection profile

Figure 24 displays the tip deflection at the end wall of the structure, which is calculated based on the horizontal displacements readings on Figure 25. The graphic illustration of the deformation is shown in Figure 26. The overall deformation occurs with a high degree of linearity initially up until roughly 8 degrees of deflection angle and a temperature of 33 degrees Celsius. Beyond this point deformation behavior rapidly transits to highly nonlinear with strong concave characteristics.

Figure 27 displays the temperature variation in the Nitinol spring triggered by Joule's heating at a constant current of 0.6A. The ambient temperature at the time was kept constant at 20 degrees and the joules heating cause a concave characteristic raise in temperature to 35 degrees over a period of 35 seconds. Over the same period the voltage reading across the Nitinol spring is displayed in Figure 28, the mean voltage reading suffered a slight decrease due to the increase in resistance, which is a coupled effect due to the increase in temperature and the partial phase transformation in Nitinol.

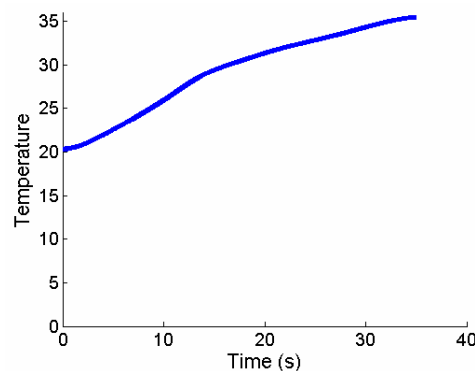


Figure 27 Temperature variation of Nitinol spring due to Joule's heating

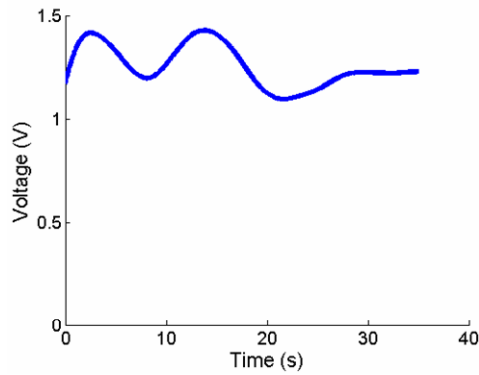


Figure 28 Voltage across Nitinol spring during actuation

The significant deflection angle achieved in this experiment was reasonably satisfying. From 2-D computational aerodynamic analysis, a typical transport aircraft traveling at transonic and subsonic conditions with airfoils that have smooth and gapless surfaces can have trailing edge deflection angles around 15 degrees before suffering from flow separation. The deflection angle achieved in the experiment was significant to clearly illustrate the major mechanism in the compliant structure in motion for the naked eye which could be an alternative into the future design of compliant airfoil structures. In addition, there is the distinct possibility that greater deflection angles can be achieved under a higher actuation current. From information provided by Images SI Inc the Nitinol spring actuators has a phase transition temperature of up to 55 degrees Celsius, which indicates the potential work capacity of the actuators was only partially deployed in this experiment as the temperature was only elevated to 35 degrees. The reason for the conservative nature of this experiment was due to the yield strain of the polycarbonate structure, from preliminary finite element analysis the maximum deflection angle achievable without suffering from plastic yielding was between 9 to 10 degrees and great caution was taken in the experiment not to place the structure under plastic yielding.

5 Conclusions

Topology optimization of compliant unit cell structures has been conducted, with the prototyping and preliminary demonstrative testing have been completed. The topology optimization featured a multi-physical system with bi-material structural composition with one passive material and one smart material that is mechanically sensitive to thermal actuation thus behaves as the actuation system. The design objective was to design the structure for the dual purpose of resisting external airload and accommodate internal actuation. The external loading was based on artificial aerodynamic loading scenario with direct loading and bending considerations. This research shows that topology optimization under multi-objective consideration can be used in the design of compliant airfoil structures, and the resulting structure is shown in lab demonstration to function according to its design; so far, under the compliant structure built with polycarbonate host structure coupled with SMA spring actuators, deflection angle of approximately 9 degrees can be achieved.

The research also indicates that significant post processing is required on the resulting topology to account for design factors that are yet difficult to express mathematically or too computationally cost to proceed. This could be a major factor in the focus of future research.

Reference

- Allaire, G., F. Jouve, et al. (2004). "Structural optimization using sensitivity analysis and a level set method " Journal of Computational Physics **194**(1): 30.
- Ananthasuresh, G. K., S. Kota, et al. (1994). A methodical approach to the design of compliant micro-mechanisms. Solid-State Sensor and Actuator Workshop.
- Bendsoe, M. P. and N. Kikuchi (1988). "Generating optimal topology in structural design using a homogenization method." Computer methods in Applied Mechanics and Engineering **71**(2): 27.
- Bendsoe, M. P. and O. Sigmund (1999). "Material interpolation schemes in topology optimization." Archieve of Applied Mechanics **69**: 19.
- Bruns, T. E. and D. A. Tortorelli (2001). "Topology optimization of nonlinear elastic structures and compliant mechanisms." Structural and Multidisciplinary Optimization **20**: 10.
- Campanile, L. F. and S. Anders (2005). "Aerodynamic and aeroelastic amplification in adaptive belt-rib airfoils." Aerospace science and technology **9**: 8.
- Canfield, S. and M. Frecker (2000). "Topology optimization of compliant mechanical amplifiers for piezoelectric actuators." Structural and Multidisciplinary Optimization **122**(2): 9.
- Chen, W., A. Sahai, et al. (2000). "Exploration of the effectiveness of physical programming in robust design." Journal of Mechanical Design **122**(2): 9.
- Cho, J. D. B., D. P. Wong, et al. (2004). "Development of high rate, adaptive trailing edge control surface for the Smart Wing Phase 2 wind tunnel model." Journal of intelligent material systems and structures **15**(279): 12.
- Frecker, M., G. K. Ananthasuresh, et al. (1997). "Topological synthesis of compliant mechanisms using multicriteria optimization." Journal of Mechanical Design **119**(2): 7.
- Howell, L. L. (2001). Compliant mechanisms New Yourk, John Wiley and Sons, Inc.
- Hutchinson, R. G., N. Wicks, et al. (2003). "Kagome plate structures for actuation." International Journal of Solids and Structures **40**: 11.
- Kota, S., K. J. Lu, et al. (2005). "Design and application of compliant mechanisms using surgical tools." Journal of Biomechanical Engineering **127**(6): 8.
- Lau, G. K., H. Du, et al. (2001). "Use of functional specifications as objective functions in topological optimization of compliant mechanism." Computer methods in Applied Mechanics and Engineering **190**: 12.
- Luo, Z., L. Tong, et al. (2007). "Shape and topology optimization of compliant mechanisms using a parameterization level set method." Journal of Computational Physics **227**(1): 25.
- Luo, Z., J. Z. Yang, et al. (2006). "A new procedure for continuum topology optimization of aerodynamic missile design." Aerospace Science and Technology **10**: 9.
- Marler, R. T. and J. A. Arora (2004). "Survey of multi-objective optimization methods for engineering." Structural and Multidisciplinary Optimization **26**(6): 26.
- Maute, K. and M. Allen (2004). "Conceptual design of aeroelastic structures by topology optimization." Structural and Multidisciplinary Optimization **27**: 15.
- Messac, A. (1996). "Physical programming: effective optimization for computation design." AIAA **34**(1): 9.
- Messac, A., S. V. Dessel, et al. (2004). "Optimization of large scale rigidified inflatable structures for housing using physical programming." Structural and Multidisciplinary Optimization **26**(1): 12.

- Messac, A. and B. H. Wilson (1998). "Physical programming for computational control." AIAA **36**(2): 7.
- Munday, D. and J. Jacob (2001). Active control of separation on a wing with conformable camber. 39th AIAA Aerospace and science meeting and exhibit.
- Nishiwake, S., M. Frecker, et al. (1998). "Topology optimization of compliant mechanisms using the homogenization method." International Journal for Numerical Methods in Engineering **42**(3): 24.
- Rahmatalla, S. and C. C. Swan (2005). "Sparse monolithic compliant mechanisms using continuum structural topology optimization." International Journal for Numerical Methods in Engineering **62**(1): 26.
- Raja, S. and A. R. Upadhyaya (2007). "Active control of wing flutter using piezoactuated surface." Journal of aircraft **44**(1): 10.
- Ramrakhiani, D. S., G. A. Lesieutre, et al. (2005). "Aircraft structural morphing using tendon actuated compliant cellular trusses." Journal of aircraft **42**(6): 7.
- Rozvany, G. I. N. (2001). "Aim, scope, methods, history and unified terminology of computer aided topology optimization in structural mechanisms." Structural and Multidisciplinary Optimization **21**(2): 18.
- Saxena, A. and G. K. Ananthasuresh (2000). "On an optimal property of compliant mechanisms." Structural and Multidisciplinary Optimization **19**(13): 36.
- Sigmund, O. (1997). "On the design of compliant mechanisms using topology optimization." Mechanism of Structures and Machines **25**(4): 31.
- Stanewsky, E. (2001). "Adaptive wing and flow control technology." Progress in Aerospace Sciences **37**: 64.
- Svanberg, K. (1995). A globally convergent version of MMA without linesearch. WCSMO-1 Proceedings of the First World Congress of Structural and Multidisciplinary Optimization, Structural and Multidisciplinary Optimization
- Svanberg, K. (2002). "A class of globally convergent optimization methods based on conservative convex separable approximations." Journal of Optimization **12**(2): 18.
- Symons, D. D., R. G. Hutchinson, et al. (2005). "Actuation of the Kagome double layer grid part 1: Prediction of performance of the perfect structure." Journal of Mechanics and Physics of Solids **53**: 19.
- Tai, K. and J. Prasad (2007). "Target matching test problem for multiobjective topology optimization using genetic algorithms." Structural and Multidisciplinary Optimization **34**(4): 12.
- Tang, W. Y., L. Tong, et al. (2005). "Improved genetics algorithm for design optimization of truss structures with size shape and topology variables." International Journal for Numerical Methods in Engineering **62**(13): 25.
- Wang, M. Y., X. M. Wang, et al. (2003). "A level set method for structural topology optimization." Computer methods in Applied Mechanics and Engineering **192**: 19.
- Xie, Y. M. and G. P. Steven (1993). "A simple evolutionary procedure for structural optimization." Computers and Structures **49**(5): 11.
- Yin, L. and G. K. Ananthasuresh (2003). "Design of distributed compliant mechanisms." Mechanics Based Design of Structures and Machines **31**(2): 28.
- Zhou, M. and G. I. N. Rozvany (1991). "The COC algorithm part II: topological, geometry and generalized shape optimization." Computer methods in Applied Mechanics and Engineering **89**: 27.